

# **VECTOR CONTROL OF ACTIVE FRONT-END CONVERTERS**

A

Major Project Report

*Submitted in Partial Fulfillment of the Requirements for the Degree*

of

**Bachelor of Technology**

in

**Electrical Engineering**

**Submitted By:**

Dhruv Parikh (15BEE068)

Varun B Sanghvi (15BEE120)

**Under Guidance of:**

**Dr. M. T. Shah**



**Department of Electrical Engineering**

School of Engineering, Institute of Technology, Nirma University,  
Ahmedabad – 382481

May 2019



**INSTITUTE OF TECHNOLOGY  
NIRMA UNIVERSITY  
DEPARTMENT OF ELECTRICAL ENGINEERING  
AHMEDABAD – 382481**

## **CERTIFICATE**

THIS IS TO CERTIFY THAT THE MAJOR PROJECT REPORT ENTITLED “ **VECTOR  
CONTROL OF ACTIVE FRONT END CONVERTERS** ” SUBMITTED BY MR.  
**DHRUV PARIKH (15BEE068) AND VARUN SANGHVI (15BEE120)**

TOWARDS THE PARTIAL FULFILLMENT OF THE REQUIREMENTS FOR THE AWARD OF THE DEGREE IN **BACHELOR OF TECHNOLOGY (ELECTRICAL ENGINEERING)** OF **NIRMA UNIVERSITY** IS THE RECORD OF WORK CARRIED OUT BY HIM/HER UNDER MY/OUR SUPERVISION AND GUIDANCE. THE WORK SUBMITTED HAS IN OUR OPINION REACHED A LEVEL REQUIRED FOR BEING ACCEPTED FOR EXAMINATION.

DATE: 10<sup>TH</sup> MAY, 2019

**INSTITUTE – GUIDE**  
**DR. M.T. SHAH**  
DEPARTMENT OF ELECTRICAL ENGINEERING  
SCHOOL OF ENGINEERING,  
INSTITUTE OF TECHNOLOGY  
NIRMA UNIVERSITY

**HEAD OF DEPARTMENT**  
DEPARTMENT OF ELECTRICAL ENGINEERING  
SCHOOL OF ENGINEERING,  
INSTITUTE OF TECHNOLOGY  
NIRMA UNIVERSITY

## ACKNOWLEDGEMENT

We must acknowledge the strength, energy and patience that almighty **GOD** bestowed upon us to start & accomplish this work with the support of all concerned, a few of them we are trying to name hereunder.

We would like to express our deep sense of gratitude to *our Supervisor Dr. M. T. Shah, Professor Electrical Engineering Department* for her valuable guidance and motivation throughout our study.

We would like to express our sincere respect and profound gratitude to **Dr. S. C. Vora, Professor & Head of Electrical Engineering Department** for supporting and providing the facilities for our minor project work.

We would also like to thank all our friends who have helped us directly or indirectly for the completion of our minor project.

No words are adequate to express our indebtedness to our parents and for their blessings and good wishes. To them we bow in the deepest reverence.

- Dhruv Parikh (15BEE068)  
- Varun Sanghvi (15BEE120)

## **Undertaking for Originality of the Work**

We, **Dhruv Parikh, Roll No.15BEE068** and **Varun Sanghvi, Roll No. 15BEE120** give undertaking that the Major Project entitled “**Vector Control of Active Front End Converter**” submitted by us, towards the partial fulfillment of the requirements for the degree of **Bachelor of Technology in Electrical Engineering at Department of Electrical Engineering, Nirma University, Ahmedabad**, is the original work carried out by us and we give assurance that no attempt of plagiarism has been made. We understand that in the event of any similarity found subsequently with any other published work or any project report elsewhere; it will result in severe disciplinary action.

---

**Dhruv Parikh**

---

**Varun Sanghvi**

**Date: 10<sup>th</sup> May, 2019**

**Place: Institute of Technology, Nirma University, Ahmedabad**

**Endorsed by:**

---

**(Signature of Internal Guide)**

**Dr. M.T. Shah**

## ABSTRACT

The current project, Vector Control of Active Front End Converters, is based on the controlling techniques (vector based) of the Active front end line side converter which mitigates the adverse effects on the overall power system, exhibited in presence of non-linear loads. Additionally, we also combine the conventional front-end converter with various negative harmonic injecting currents converter: active filter, that in combination work efficiently to harness the best qualities of the power system. Thus, initially vector based techniques of various associated transforms and various mathematical modeling of such converter-based systems is studied in depth, subsequent to which the study of these specific topologies is done. A simulation is done so as to implement the topology of a front-end converter simultaneously acting as an Active Filter. Concepts of Adaptive Gain control are implemented so as to keep the currents in the limits of the utilized power electronic switches. A closed loop current feedback control is implemented, utilizing the techniques of Hysteresis Current Control as well as Adaptive Hysteresis Current Control. The load connected is a SPWM controlled inverter -based Induction motor to verify the algorithms to industrial standards. Disadvantages of Adaptive Hysteresis methods have been discussed and in order to cope with them another novel strategy is implemented – Hexagonal Hysteresis Current Control. A comparative analysis has been done to understand the various positive and negative aspects of all the strategies.

**Keywords:** Power Electronic Converters, Active Front End Converters, Vector Control, Active Filter, Adaptive Gain Control, Hysteresis Controller, Adaptive Hysteresis Controller, Hexagon-based predictive hysteresis controller; Comparative Analysis;

# TABLE OF CONTENTS

<b>ACKNOWLEDGEMENT</b>	iii
<b>UNDERTAKING FOR ORIGINALITY OF WORK</b>	iv
<b>ABSTRACT</b>	v
<b>TABLE OF CONTENTS</b>	vi
<b>LIST OF FIGURES</b>	vii
<b>LIST OF TABLES</b>	viii
<b>NOMENCLATURE/ABBREVIATIONS</b>	ix
<b>CONTENT</b>	
<b>CHAPTER 1: INTRODUCTION</b>	01
1.1 Introduction	01
1.2 Inspiration behind the Project	02
1.3 Objective of the Project	03
1.4 Literature Review	04
1.5 Types of Power Quality Conditioners	05
1.5.1 Shunt Active Filter	
1.5.2 Series Active Filter	
1.5.3 Hybrid Filter	
1.6 Reason to use AFE in Simultaneously as SAPF	06
<b>CHAPTER 2: ACTIVE FRONT END CONVERTERS</b>	07
2.1 Introductory Aspects	07
2.2 Converter Simultaneously as Active Front End Converter and Active Filter	08
2.3 Circuit's Mathematical Model & Relevant Equations	09
2.4 Park's Transform: The d-q model of an Induction Machine	
<b>CHAPTER 3: VECTOR CONTROL TECHNIQUES</b>	10
3.1 Operation of the PWM Front End Converter	10
3.2 Instantaneous Power Theory (p-q theory)	10
3.3 Power Flow Control Strategy	12
3.4 The Adaptive Gain Control scheme	14
3.5 Compensating Reference Current Generation	17
<b>CHAPTER 4. CURRENT CONTROL STRATEGIES</b>	18
4.1 Advantages of current- controlled PWM converters:	19
4.2 Hysteresis Current Controller – Delta Modulation controller	19
4.3 Disadvantages of Nominal Hysteresis Regulator	21
4.4 Adaptive Hysteresis based current controller	21
4.5 Current Error Space Phasor based Hexagonal Hysteresis Controller	25

	4.5.1	Introduction	25
	4.5.2	Principle of Hexagon Hysteresis Control	27
	4.5.3	Structure of hysteresis control	28
	4.5.4	Principle adopted for Switching Sequence Generation	29
	4.5.5	Switching Table	29
<b>CHAPTER 5: CIRCUIT IMPLEMENTATION IN MATLAB/SIMULINK</b>			30
5.1	CIRCUIT PARTS		30
	5.1.1	PI Controller – DC Link Voltage	30
	5.1.2	Load Side Converter	30
	5.1.3	Control of Inverter – SPWM	31
	5.1.4	Main Load Connected	31
	5.1.5	Operation in transient condition	31
5.2	Design Specifications and Circuit Parameters – Adaptive Hysteresis:		32
5.3	Design Specifications and Circuit Parameters – Hexagon based Hysteresis Controller		32
<b>CHAPTER 6: SIMULATION RESULTS</b>			
6.1.	Fixed Band based Hysteresis Current Controller		33
6.2	Adaptive Band based Hysteresis Controller:		36
6.3	Current Error based (Hexagonal Band) Current Controller		40
<b>CHAPTER 7: COMPARATIVE ANALYSIS</b>			43
7.1	Line Regulation		43
7.2	Load Regulation		44
7.3	THD Comparison for various control techniques		47
<b>CHAPTER 6: Conclusion and Future Scope of the Project</b>			48
<b>REFERENCES</b>			49

## LIST OF TABLES

<b>Table No:</b>	<b>Name of the Table</b>	<b>Page No:</b>
1	On/Off output states of three-phase VSI.	30
2	Switching Table for Hexagonal Band Hysteresis controller.	32
3	Dynamic Switching.	32
4	Design Specifications	34
5	Comparison of THD values	47

## LIST OF FIGURES

<b>Fig No:</b>	<b>Name of the Figure:</b>	<b>Page No:</b>
Fig.1.1	Windings of Induction Machine	3
Fig.1.2	abc-d <sub>s</sub> -q <sub>s</sub> transform	4
Fig.1.3	d-q axis transforms of the winding emfs	5
Fig.1.4	d <sub>s</sub> -q <sub>s</sub> equivalent circuit	6
Fig.1.5	Current and Flux vectors in Induction-Machine	7
Fig.2.1	Block Diagram of Active Power Filter	8
Fig.2.2	Basic Circuit Configuration of Shunt Active Filter	9
Fig.2.3	Equivalent Circuit	10
Fig.2.4	Transform diagrams	11
Fig.3.1	The Generic Front-End Converter with Non-Linear Load	12
Fig.3.2	Simplified Model of the main load side of the Converter	13
Fig.3.3	Overall schematic of Control Scheme	13
Fig.3.4	Adaptive Control of Gain	15
Fig.3.5	Algorithm	17
Fig.3.6	Reference current generation Block	18
Fig.4.1	Block diagram of current controlled PWM converter	19
Fig.4.2	Addition possibilities of different voltage vectors and production of same output vector.	21
Fig.4.3	Hysteresis bands for three phase reference currents	23
Fig.4.4	Switching when upper and lower hysteresis band is reached.	24
Fig.4.5	Power Circuit Topology	24
Fig.4.6	Switching states of VSI output voltages. Reference voltage present in sector S <sub>1</sub> .	25
Fig.4.7	Hysteresis Hexagon in ( $\alpha$ , $\beta$ ) plane. Current error phasor presents in sector S <sub>I</sub> .	26
Fig.4.8	General Schematic of Hysteresis Control.	28
Fig.4.9	Hatched areas A <sub>0</sub> , A <sub>3</sub> , A <sub>4</sub> and A <sub>5</sub> and bc-axis shown.	29
Fig.4.10	Hatched areas A <sub>0</sub> , A <sub>4</sub> , A <sub>5</sub> and A <sub>6</sub> and ab-axis shown.	29
Fig.4.11	Stationary and Dynamic Hysteresis Hexagon.	30
Fig.5.1	DC Link	30
Fig.5.2	Load End Converter	31
Fig.5.3	SPWM technique used to trigger the Inverter.	31
Fig.5.4	3 - $\Phi$ Induction Motor connected as a primary load.	31
Fig.5.5	Complete Simulation Circuit in MATLAB/Simulink Environment	32
Fig. 6.1.1	Supply current waveform	34
Fig. 6.1.2	Measured current vs Reference current	36
Fig. 6.1.3	Adaptive Gain Algorithm Output	37
Fig. 6.2.1	Supply current waveform	39
Fig. 6.2.2	Measured current vs Reference current	39
Fig. 6.2.3	Adaptive Hysteresis Band for phase A	40
Fig. 6.2.3	Electromagnetic Torque	41
Fig. 6.2.4	DC Link Voltage Profile.	41
Fig. 6.2.5	Supply Voltage & Current waveform – UPF Operation.	42



Fig. 6.3.1	Supply Current Waveform (a-phase)	43
Fig. 6.3.2	XY Plot of $i_{e\alpha}$ (x-axis) and $i_{e\beta}$ (y-beta) – Hexagonal Hysteresis Band.	43
Fig. 6.3.3	Line Voltage Waveform.	44
Fig. 6.3.4	(a) DC Link Voltage Profile	44
Fig. 6.3.4	(b) DC Link voltage after settling time	45
Fig. 6.3.5	Load Torque Variation at $t = 2$ sec.	45
Fig. 6.3.6	Unity Power Factor Operation	46
Fig. 6.3.7	Three phase Sinusoidal reference currents when the mode of operation is changed from AFE mode to Simultaneous operation as AFE and SAPF	46
Fig. 7.1	Total Harmonic Distortion for Conventional Hysteresis	47
	(a) AFE Mode – 2.44% (b) Simultaneous Mode - 6.11%	47
Fig.7.2	Total Harmonic Distortion for Adaptive Hysteresis	48
	(a) AFE mode (b) Simultaneous Mode	48
Fig. 7.3	Total Harmonic Distortion for Hexagonal Hysteresis	49
	(a) AFE mode – 2.01 % (b) Simultaneous Mode – 5.79%	49

## NOMENCLATURE/ ABBREVIATIONS:

Sr. No.	Symbol/Abbreviation	Full form
1	$\Omega$	Ohm
2	F	Farad
3	A	Ampere
4	V	Voltage
5	RMS	Root mean square
6	W	Watt
7	PWM	Pulse width modulation
8	IM	Induction motor
9	DTC	Direct torque control
10	HB	Hysteresis Band
11	PID	Proportional-Integral-Derivative
12	FOC	Field oriented control
13	KCL	Kirchhoff's current law
14	HCC	Hysteresis Current Controller
15	AHCC	Adaptive Hysteresis Current Controller
16	$\omega$	Frequency (omega)
17	$\Theta$	Theta – angle
18	$\alpha$	Alpha (axis)
19	$\beta$	Beta (axis)
20	s	Laplacian Operator
21	$i_a, i_b, i_c$ .	Supply Currents
22	$i_e$	Error Current
23	$i_{ref}$	Reference Current
24	AFE	Active Front-End
25	SAPF	Shunt Active Power Filter

# **CHAPTER 1: INTRODUCTION**

## **1.1 Introduction**

In the current era, with the advent of electronic devices and traditional electrical systems operated via switching of various power electronic devices, both at the industrial level with extremely high values of loadings and at the domestic and commercial level with an equally large proportion of non-linear loads connected to the grid, it becomes imperative to solve the problem of harmonics in the current drawn by these loads, as in lieu of such a problem solving tactic there occurs a situation where large non-linear currents drawn from the grid by the load, effectively comprises the voltage waveform available at various other loading portions in the power network.

Power Quality has been continuously degrading since the penetration of Electronics at a large scale – there has been a significant increase in harmonic pollution due to the penetration of non-linear loads. The presence of PWM techniques have made it possible to control the operation of converters in such a manner so as to control the flow of active and reactive power, thereby controlling the parameters of torque and flux.

## **1.2 Inspiration behind this Project:**

The problems posed by the penetrated electronic loads, effectively deteriorates the performance of both linear and non-linear loads creating an effective non-sinusoidal behavior in the entire power network. This deterioration then is responsible for a huge range of problems:

The harmonic composed voltages when supplicated to an IM effectively forces a relatively non-sinusoidal current through the IM which results in torque pulsations which affect the performance of the IM and the loads that it drives.

Harmonic components of currents result in unnecessary and wasteful heating of a major portions of load, thus making the system more loss producing.

For the same amount of active power drawn, obviously, with the presence of harmonic components, effectively, a higher amount of total RMS current flows through the power lines resulting in a higher proportion of line losses.

Harmonic distortion in current generates a harmonic distortion in the supply voltage and pollutes the supply voltage and its waveform that are driving numerous other loads which depend on the sinusoidal characteristics of the input voltage to a certain extent.

The major impact of harmonics thus as seen above, is not just limited to its impacts on all the other loads that are being driven with a distorted voltage waveform, but also in the performance debilitation of an IM which comprises of major proportion of load all over the world.

Thus, the major impetus of solving this problem appears in the generality of it, and in the rate with which non-linear loads are increasing. A front-end converter is connected at the line side and helps in locally ensuring that irrespective of the connected load in the system from the

supply, an interface of an inverter ensures that it corrects the non-linearity that the non-linear loads induce in the supply network at the local supply points from wherein the load is connected.

In addition to this in a network where the load circuit is irreplaceable and where the load network can't be modified to accommodate an AFE, a connection of a shunt connected power filter induces a current in the network that reduces the harmonics at the supply side to null. However, our motivation for the project led us to a system wherein the front-end converter, once connected to the system, also takes care of loads connected in shunt with the power lines at the PCC. Thus, the front-end converter connected at the line side also acts as a SAPF, simultaneously reducing harmonics due to both the shunt and the AFE connected load at the line side. Simultaneous operation is possible, and so is individual operation as an AFE and an SAPF. The reduction in THD in the non-simultaneous and the simultaneous operation is remarkable for a huge array of loads.

Additionally, to ensure that no matter how much load is connected either in shunt or in the AFE side, the IGBT switches mustn't be damaged, an additional logic of adaptive gain has been used which reduces the compensating powers when the d-q axis currents exceed the maximum limit thus forcing the reference within the limits of the IGBT switch.

Also, the controller used in the beginning was a normal hysteresis controller with fixed hysteresis bands, post which the utilization of hysteresis bands with adaptive band width was done to obtain a set limit on the maximum switching frequency. Thus, both normal and adaptive hysteresis controllers have been tested with their outputs obtained. Finally, a hexagonal hysteresis controller based on SVPWM switching of the inverter legs was also simulated and the hardware implementation of the same was seen.

The various problems in each controller, advantages of each and the parameter comparison of each was done in addition to a comparison of the outputs obtained in each one of the simulated controllers and a validation of the obtained simulated output was also done using the hardware implementation of the hexagonal hysteresis controller.

### **1.3 Objectives of the Project:**

1. Understand the various techniques of vector control along with various transform techniques that are utilized in these control strategies and to implement them for the control of a front end converter.
2. Understand, simulate and design the simultaneous operation of converter as an Active Front-End as well as an Active Power Filter and obtain the effects it has on the supply current waveform, it's THD and also the effects on the DC link voltage due to the presence of the load on the AFE side
3. Understand and Implement the Instantaneous Power Theory (p-q theory), hence utilizing it to obtain the reference compensating currents ( $\alpha\beta$  frame) and subsequently converting it to abc reference frame.

4. Analyze the significance of Adaptive Gain Controller to keep the measured values of currents within the limits of the utilized power electronic switches.
5. Implementation of Hysteresis Current controller strategy to produce the PWM gating pulses; understanding the importance, advantages as well as disadvantages of the HCC controller, and recognizing the simplicity of its implementation.
6. Implementation of an Adaptive Hysteresis Current Controller (AHCC), wherein the hysteresis band varies as a function of load parameters keeping the switching frequency almost constant. Acutely observing the many advantages in terms of its dominance in analysis of harmonic Spectrum, and reduction of lower order harmonics.
7. Comparative Analysis of HCC and AHCC in terms of its advantageous operation at a constant switching frequency, by reduction of switching losses as well as lower THD levels.
8. Understanding the problem of current- error leading to a peaky- waveform, thereby reducing the quality of AHCC. Subjectively tracking down the reason for such problem, analyzing it from the perspective of actual current being unable to follow the reference current. Implementing the Hexagon-type predictive current controller to reduce the peaks present in waveform.
9. Utilize a novel SVPWM switching technique to obtain the current error within the required margins using a hexagonal current error region, along with a look up table of switching states based on the location of reference voltage and the current error, by selecting a switching state which aids in bringing the current error back to zero by a specific current error derivative vector in direct opposition to the current error obtained.
10. A final comparison of the above techniques; HCC, AHCC and Hexagonal SVPWM CC; in terms of various parameters like THD, DC link voltage stabilization, current error control, matching between the reference and the actual current, switching frequency of the switch, among others.
11. Hardware implementation of the Hexagonal Current Error SVPWM CC in the circuit topology that control both the line side harmonics injected due to the switching of the load via a capacitor connected on the converter side and also the injection of harmonics due to the non-linear load connected across the converter, acting as a power filter, for the shunt connected load, both simultaneously; the simultaneous operation does not preclude the possibility of non-simultaneous or individualized operation as such, however for implementation simplicity, only a load on the front end side excluding the shunt connected load may be utilized rather than the entirety of the power circuit; again the entire power circuit however, has been simulated in MATLAB Simulink nonetheless.

## 1.4 LITERATURE REVIEW:

[1] *B. K. Bose Modern Power Electronics and AC Drives (Book)*

This particular text was utilized to understand the fundamentals of vector-based controllers and various transforms like the abc to alpha-beta-zero and the alpha-beta-zero to dq. Additionally, modeling of a basic Induction Motor (squirrel cage type) was also understood for better understanding the modeling of electrical systems in the alpha-beta-zero and the dq reference frames.

Additionally, this text helped in the basic foundation of the equation transformation from one particular system to the other. Chapter-2 of the text dealt with these topics in detail and were referred by us for the basic idea regarding various transform systems and their applied utility in analyzing electrical systems.

[2] *Control of front-end Converter with Shunt active Filter using adaptive gain Hong Viet Luu Alfred Punzet, Volkmar Müller, Ngoc Lan Phung, DRESDEN UNIVERSITY OF TECHNOLOGY Mommsen Strasse 13, D-01062 Dresden, Germany. ISBN: 90-75815-08-5. (Paper)*

This paper formed the basis of our control circuit in its initial stages; this paper introduced us to the concept of harmonic compensation using a current controller whereby the reference currents are generated utilizing p-q theory of compensation as proposed by Akagi. Additionally the adaptive gain algorithm utilized in this paper has also been utilized in our circuit topology to obtain a gain constant K that regulates the extent to which the compensating powers are compensated in the form of compensating currents, to ensure that irrespective of simultaneous AFE and SAPF loading.

There still exists a marked degree of safety for the IGBT's of the AFE inverter circuit, obviously the first level of safety here would be to pre-mention the loading limits at both the front end side and the SAPF side, however assuming that the supply point can accommodate numerous shunt connected loads, the adaptive gain concept adds in on the factor of safety over and above the safety provided using the load specification and load limitation.

This paper used a generic current controller and, in the project, a normal hysteresis controller was utilized by us to obtain the output of this particular circuit topology. A variation in load effected a reduction in K from 1 towards values in the range of 0.8-0.9 to ensure safe operation of the IGBT's in the inverter circuit.

[3] *Converter Simultaneously as Active Front End and as Active Filter, A. Ndokaj and A. Di Napoli Roma Tre University, Dept. of Ind. and Mecc. Engineering, (Italy), 978-1-4673-4430-2/13/\$31.00 ©2013 IEEE. (Paper)*

This paper introduced us to the concept of operating a front end simultaneously as a front end and as a SAPF to reduce the harmonics at the line side. This paper was based on a different compensation theory; the dq park transform theory that even though wasn't implemented in our simulations helped the understanding and the comparisons of various reference current generating strategies.

[4] *Modelling and Analysis of Electrical Machines* by Mrityunjay Bhattacharyya (Book)

This text again helped understand the basics of the various transform techniques in electrical systems. Additionally, difference between active and passive transforms, its utility, among other things were understood in this text.

[5] *Vector control of three-phase AC/DC front-end converter*, J S SIVA PRASAD, TUSHAR BHAVSAR, RAJESH GHOSH and G NARAYANAN Department of Electrical Engineering, Indian Institute of Science, Bangalore 560 012. *Sadhana* Vol. 33, Part 5, October 2008, pp. 591–613. (Paper)

This paper again introduced the various introductory aspects of an AFE and its control strategies based on the various basics associated with a front-end converter topology. The generation of the AFE three phase reference current, and its switching, either using the voltage based switching techniques or using the current controllers was discussed in this paper. Unit vector generation, feed forward compensation, switching of various output voltages, operation as an inverter or rectifier were the topics of major relevance studied in this particular paper.

[6] Marian P. Kazmierkowski, Ramu Krishnan, Frede Blaabjerg, J. D. Irwin-*Control in Power Electronics Selected Problems (Academic Press Series in Engineering)* (2002)

This book introduced us to the control techniques implemented in various power electronic circuits and inverter topologies including the 2-level inverter utilized in our circuit topology.

[7] Manisha Shah, P.N Tekwani, “Current Error Space Phasor Based Hysteresis Controller Applied to Bi-Directional Front-End Boost-Converter for Unity Power Factor and Low THD

This paper talks about a slightly different type of Hexagonal Hysteresis control strategy wherein the switching states are defined not as sectors of  $60^\circ$ , but rather as regions of  $120^\circ$  each, for odd and even sectors of reference voltage vector. This methodology prevents random switching states from being triggered and a better line voltage waveform can be achieved. This particular paper has a control strategy quite alike the control strategy that has been utilized, however is different in the aspect of not having a dynamic switching table which takes care of extreme current excursions.

[8] *Instantaneous Power Theory and Applications to Power Conditioning* H. Akagi, E. H. Watanabe, M. Aredes

This text introduces the concept of p-q theory of power compensation to obtain sinusoidal voltages and currents in the network. This theory, developed by Akagi and dealt with in detail in this text gives a detailed understanding of the physicality of the p-q theory, the p-q compensation of a harmonic riddled network, and its implementation in a AFE/SAPF based circuit. The waveform of reference currents, and its generation using a hysteresis controller along with other modified controllers based on hysteresis controller and the various methods that may be used for the reference current generation including the d-q reference frame theory and the Generalized Fryze's Theory, and their comparisons among various other theories were the relevant material of study used to understand and grasp the basis of the various theories used to simulate a FEC

working simultaneously as an SAPF. The text is detailed and gives the physical utilitarian meaning of the instantaneous p and q components of power.

The utilization of these p-q components then to obtain the appropriate reference current for harmonic elimination when working as an SAPF, SAPF and AFE simultaneously or for pure reference sine wave generation when working as an AFE are amongst the fundamentals mentioned in the book utilized in our circuit.

[9] L. Malesani, P. Mattavelli, “Novel Hysteresis Control Method for Current- Controlled Voltage-Source PWM Inverters with Constant Modulation Frequency”, *IEEE Transaction on Industry Applications*, Vol. 26, No. 1, January/February 1990., pp. 88-92

This paper discusses the application of Hysteresis controller in a generic inverter topology with additional focus in the aspects concerning the control of the modulation frequency of the IGBT switches of the inverter, specifically how to maintain an approximately constant maximum switching frequency of the IGBT switches in the inverter. Additionally, the paper focuses on reducing the non-requisite effects of inter-phase interference which affect the magnitude of the hysteresis band which has been selected and changed to ensure an approximately constant switching frequency.

In order to relinquish these problems the hysteresis band is separated into a phase independent term and a phase dependent term, and by ensuring that the phase independent term is the one that is modulated for ensuring an interference free (corresponding to reduction in spikes and reduction in the errors of the actual current tracking the reference current) operation and an operation at constant (relatively) frequency. Finally, it has been shown that despite setting only one component of the actual hysteresis band set, the other, phase interference dependent component, is also automatically set, thus not affecting the final (actual) hysteresis band region in the final control schematic.

[10] Mirjana Milosevic “Hysteresis Current Control in Three-Phase Voltage Source Inverter”

This paper talks about the advanced current control method, in which the current error space phasor in  $\alpha\beta$  frame is being controlled by a hysteresis hexagon. The author has described the principle logic behind the method of hexagonal control and has also talked about the selection of switching states. This paper explains the selection of switching vectors, based on a given sector of the current error space phasor in the alpha-beta frame, and the sector of the reference voltage vector. The reference voltage sector governs the regions in which the current error derivatives exist, which obviously differ for different switching states, but once the sector of the current error has been identified, the current error derivative must precisely be opposite to the current error to ensure that that particular switching state brings the current error back to origin, however as such, in lieu of such a precise switching state, due to its possible absence, a current error derivative sector (region) and thus a switching state corresponding to a given sector of the current error space vector is decided for both the dynamic boundary crossings and the stationary boundary crossings to ensure an appropriate output of current from the inverter, according to the reference that is generated.

## 1.5 TYPES OF POWER QUALITY CONDITIONERS

### 1. Shunt Active Power Filter

This configuration is useful for elimination of the current harmonics which are generated owing to nonlinear loads. Its usage is mostly limited to load distribution centers. The compensator, which is connected in parallel with non-linear loads. The point that combines the Shunt Filter with ac grid system is called the Point of Common Coupling (PCC). The compensators inject currents in a way to cancel out the harmonics of the load.

### 2. Series Active Power Filter

This filter is usually connected before the load serially with the mains by using a synchronized transformer. The aim is elimination of the voltage harmonics, balancing and maintenance of the terminal voltage of the load. This device, when installed helps in damping of the harmonics which are previously propagating due to resonance with line impedance and other passive shunt compensators.

### 3. Hybrid Power Filters

Hybrid Filters are advantageous in the scenario where the compensation effect is no longer under influence of the impedance of the supply. Parallel resonance, becomes a possibility between the source impedance and shunt passive LC filter disappears because of Series Active Filter. Hybrid Active Filters can combine the advantages of both passive and active filters without the involvement of any of their so stated disadvantages. These filters also have the capability of reducing the current voltage harmonics at a reasonable cost.

### 4. Unified Power Quality Conditioner (UPQC)

Unified Power Quality Conditioner, a special type of Active filter is actually a combination of Active Series and Shunt Filter. Only one dc storage capacitor is used in this topology and is installed between Active Shunt and Active Series compensator. It can also be used in single and three phase configurations. It is a power filter, which has the feature to eliminate voltage and

current harmonics. However, the major drawback is that it is expensive and its control algorithm is quite complex because of large number of switching devices involved.

*All the above-mentioned filters work in a way as to mitigate the effects of the harmonic distortion, but they do not completely eliminate it. In order to eliminate the effects completely, we need an Active Front-End converter.*



## Operation of AFE

According to current trends induction motors are connected as loads via an AC -DC Rectifier. The DC link of the rectifier goes to another load connected inverter, the control of which controls the induction motor for various speed control operation. However, the problem with simple AC-DC rectifier and phase control rectifier is that despite them creating a stable enough DC Link on the inverter, they end up injecting harmonic components on the grid-end.

These components pollute the grid supply and all the loads connected to it. These harmonic currents injected at the supply-end can be altogether eliminated by utilizing a PWM rectifier as AC-DC converter. The switching of this PWM rectifier is done so as to ensure the stability of the DC Link, all the while maintaining the sinusoidality of the supplying circuit. This switching can either be done via the pq theory which generated the reference current or via the theory of vector control which works on principle of generation of reference voltages.

### **1.6 Reasons to utilize a PWM rectifier as an AFE simultaneously acting as SAPF:**

As the major chunk of the loads connected the grid are induction motor, which with the advent of scalar and vector control techniques require a DC Link which is obtained via a line connected inverter, it isn't uncommon to see an AC-DC converter on the line side with an inverter connected load to control the motor. Thus, without adding any additional inverter circuit on the line side it is possible to reduce the grid connected harmonics by utilization of the already present AFE which also acts as a shunt active power filter for shunt connected loads.

Thus, without any additional harmonic supplying circuit, the sinusoidal operation of the grid is ensured via the action of an AC-DC PWM rectifier that supplies both the loads connected across its DC Link which simultaneously injecting the harmonic current needed by the parallel connected non-linear load.

In circuits which are not commissioned yet, an inverter is preferred, but incase of circuits having a DC Link which are converter based and already in operation by utilizing scalar control techniques, a cost-effective method is to implement the vector control for simultaneous operation.

## **CHAPTER 2: Active Front End Converter and Shunt Active Power Filter**

### **2.1 Introduction**

There are two major topologies of Active front-end converter which have been implemented in the simulation to ensure an efficient and desired operation of the converter.

- a. Converter Simultaneously as Active Front end Converter and Active Filter.
- b. Control of front-end Converter with Shunt Active Filter using Adaptive Gain.

In case of simultaneous operation, the front-end converter acts as a Shunt Active-Filter for Non-Linear load, connected in parallel to the main load [2]. The control schematic is shown in Fig. 2.1 Block Diagram. It is to be noted that the AFE itself acts as the SAPF for the harmonic producing load as depicted in Fig. 2.1

### **2.2 Converter Simultaneously as Front-End and Shunt Active Filter**

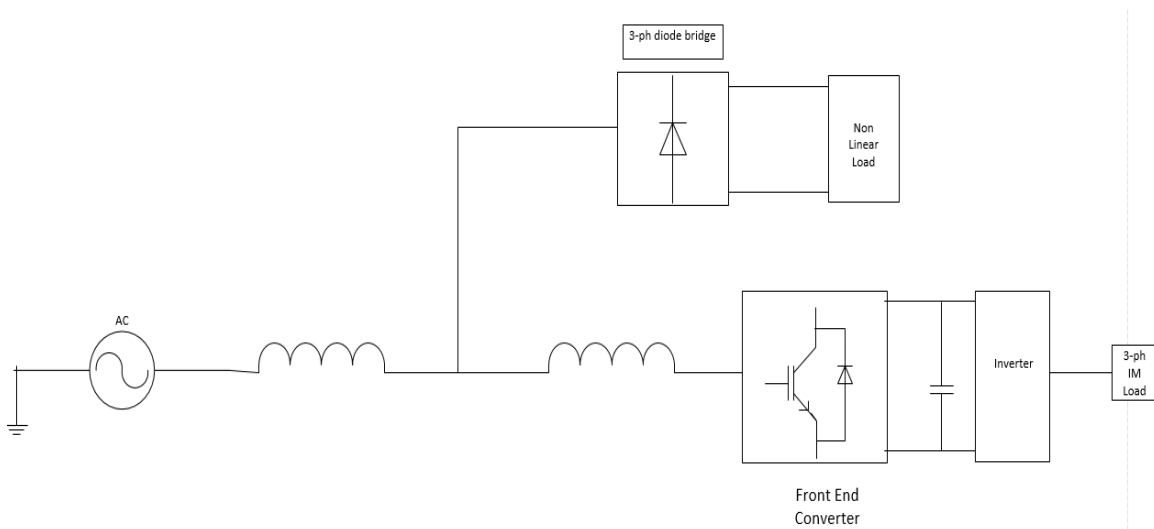


Fig. 2.1 Block Diagram of Active Power Filter

Theoretically, all the approaches should be able to solve the problem, however there are some practical constraints to be considered. For first approach, we will need additional device; and of course, additional cost will be incurred. The second approach is effective for all units; but replacement costs would be heavy. Hence here the third approach is most cost-effective and is therefore implemented.

$$i_{AF} + i_L = i_s \quad (1)$$

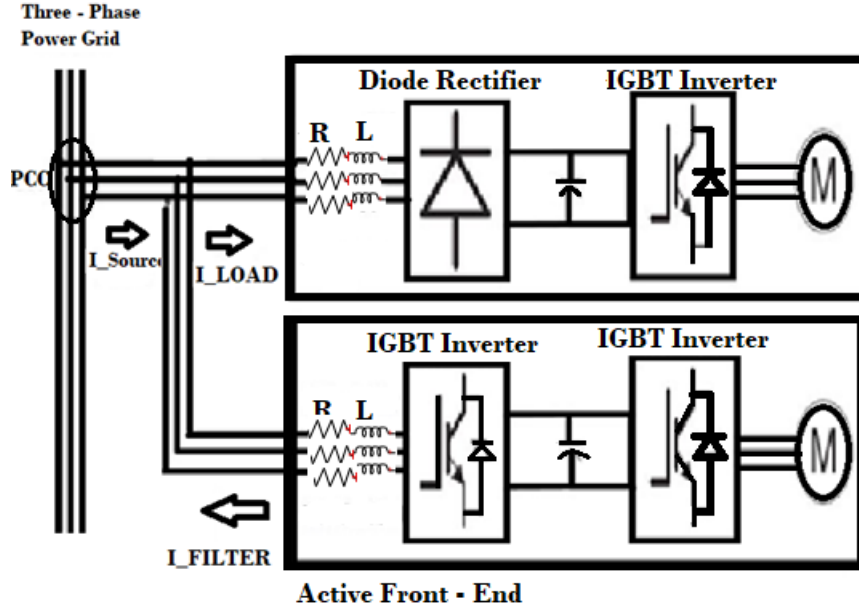


Fig 2.2 Basic Circuit Configuration of Shunt Active Filter

## 2.3 Mathematical Model of Circuit Topology

Consider the following equivalent circuit,

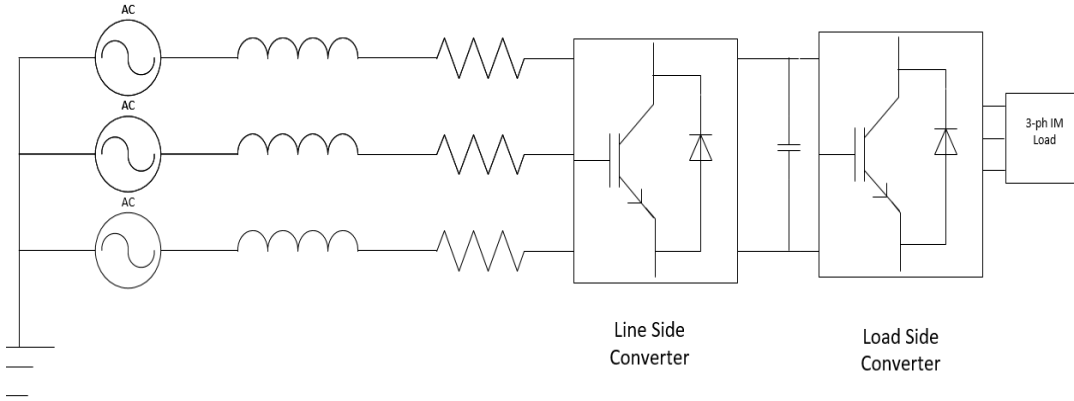


Fig 2.3 Equivalent Circuit

We know that,

$$\bullet \quad P = 3E \frac{V \sin \delta}{\omega L} \quad (1)$$

$$\bullet \quad Q = 3E \frac{V \cos \delta - E}{\omega L} \quad (2)$$

These are the basic power transfer equations for a simple balanced three phase system [4]. Based on the various transforms, the following d-q dynamic model equations of the system are:

- $E_{qe} = L \frac{di_{qe}}{dt} + \omega L_{ide} + R_{iqe} + V_{qe}$  (3)

- $E_{de} = L \frac{di_{de}}{dt} - \omega L_{iqe} + R_{ide} + V_{de}$  (4)

- $C \frac{dv}{dt} = i_{dc} - i$  (5)

### Transform Diagrams

- We have:  $\omega = \frac{d\theta}{dt}$
- The speed  $\omega$  is the frequency of the supply voltage E with which we assume the dynamic d-q axis to rotate, with a shift of  $\omega t$  in time t. Additionally, we have the following conditions imposed for relative simplicity in the control schematics:  $E_{qe} = 0$  by selecting a suitable value of  $\theta$ .
- By the generalized instantaneous power theory, it is provable that the various powers are as follows: Here the reactive power equation shows that for a positive  $i_{qe}$ ,  $Q_{de}$  is negative, implying that the rectifier feeds the reactive power back to source. and vice versa. Refer Fig 2.4. The capacitor charging equation governs the dc link voltage, with the currents shown in the diagram of Fig.2.4 quite appropriately [4].

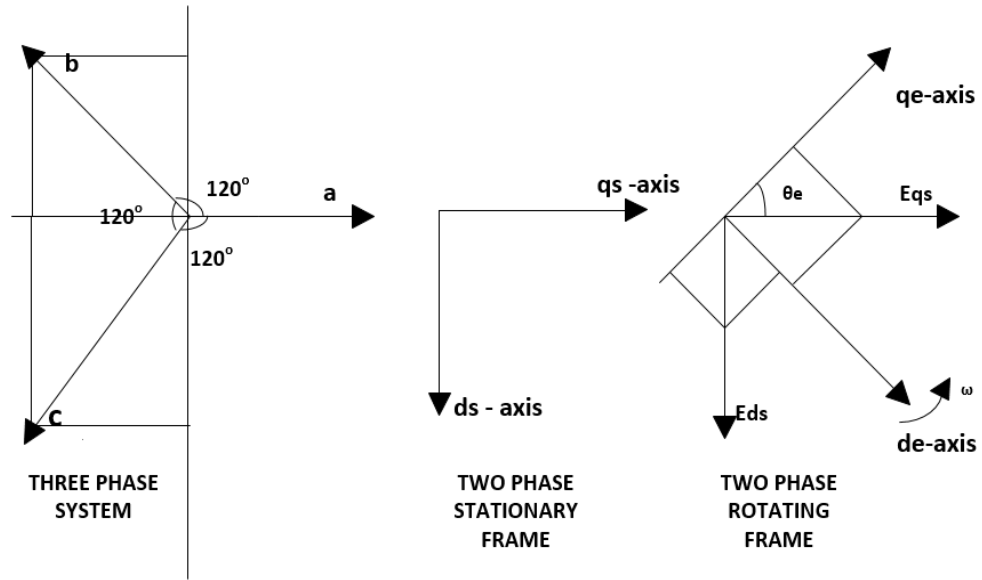


Fig 2.4 Transform diagrams

## 2.4 The Park's Transform: d-q Model of an Induction Machine

The Park's transform will be discussed in line with the d-q model of the induction machine. Once the Clark's transform has been discussed, the motivation is now to obtain the d-q machine model using Park's transform on the  $\alpha\beta\gamma$  system obtained via the Clark's transform. Discussing these transforms in line with the modeling of an induction machine we move forward. [5]

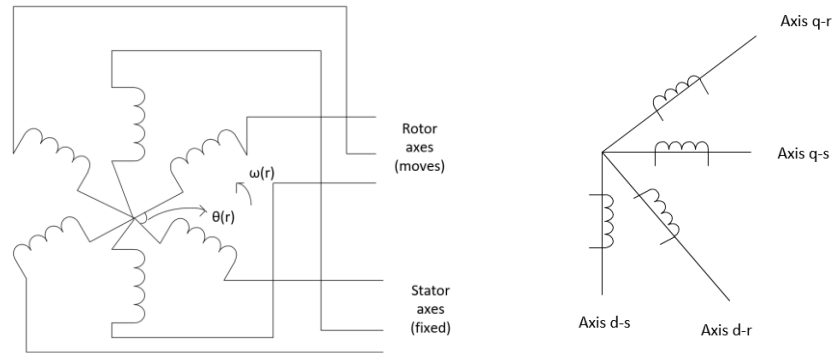


Fig 1.1 Windings of Induction Machine

As seen from the Fig.1.1 our primary goal is to convert the entire system into the following 2 phase system using the appropriate transforms. Here Park was the first one to transform the stator variables of the synchronous machine to the rotor circuit rotating at the synchronous speed.

After him Stanley transformed various variables to stationary references. Kron then suggested that it is indeed possible to simplify the equations further by utilizing a synchronously rotating reference frame. Finally, Krause suggested that actual transformations can actually be done pertaining to any arbitrarily rotating frame of reference.

### Axes Transformation

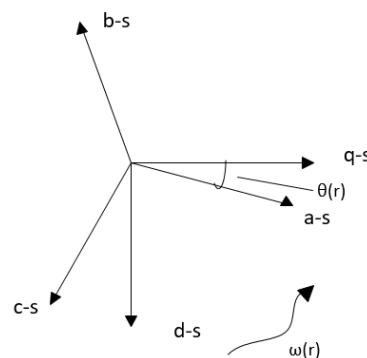


Fig 1.2 abc-ds-qs transform

Here in the axis transformation we first transform the three as-bs-cs axes into the  $d_s$ - $q_s$  axis and then to another  $d_e$ - $q_e$  axis which will complete the stator circuit transformation from the original axis to the two-phase stationary and the two phase synchronously rotating axis respectively.

$$\begin{bmatrix} v_{as} \\ v_{bs} \\ v_{cs} \end{bmatrix} = \frac{2}{3} \begin{bmatrix} \cos \theta & \sin \theta & 1 \\ \cos(\theta-120^\circ) & \cos(\theta-120^\circ) & 1 \\ \cos(\theta+120^\circ) & \cos(\theta+120^\circ) & 1 \end{bmatrix} \begin{bmatrix} v_{qs}^s \\ v_{ds}^s \\ v_{cs}^s \end{bmatrix} \quad (1)$$

$$\begin{bmatrix} v_{qs}^s \\ v_{ds}^s \\ v_{cs}^s \end{bmatrix} = \frac{2}{3} \begin{bmatrix} \cos \theta & \cos(\theta-120^\circ) & \cos(\theta+120^\circ) \\ \sin \theta & \sin(\theta-120^\circ) & \sin(\theta+120^\circ) \\ 0.5 & 0.5 & 0.5 \end{bmatrix} \begin{bmatrix} v_{as} \\ v_{bs} \\ v_{cs} \end{bmatrix} \quad (2)$$

Here  $v_{0s}$  pertains to the zero sequence components which may/may not be present.

The  $d_e$ - $q_e$  axes voltages have been obtained from the  $d_s$ - $q_s$  axis voltages.

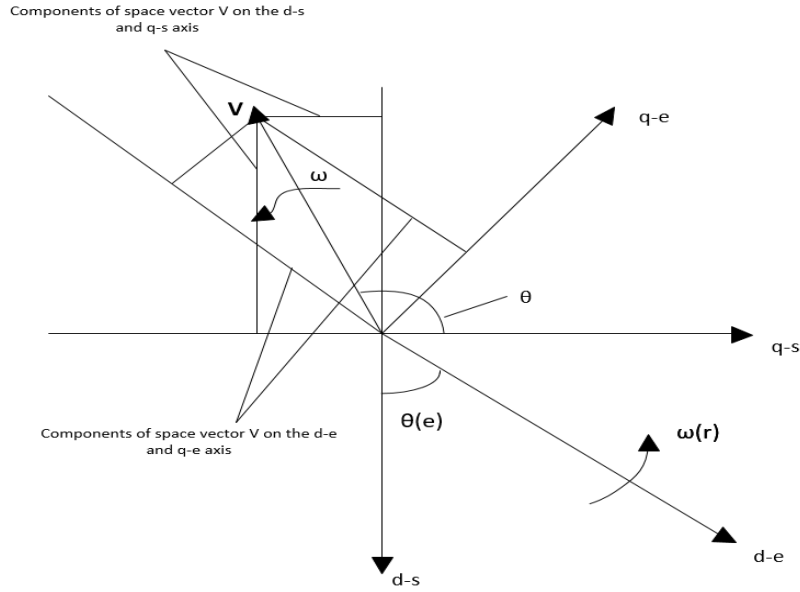


Fig. 1.3 d-q axis transform of the winding emfs

The associated equations and consolidation of the utilitarian factor of the transforms are as follows. These equations are in the synchronously rotating frame of reference. Thus, we can see that the voltages in the synchronously rotating reference frames are obtained as dc values constant. A space phasor representation of the above set (couple) of voltages is also obtained in the following fashion:

Here we have merely combined the two components of the voltages in the complex form. We can see that the vector magnitudes of the complex voltages in the corresponding reference frames are equal.

$$|V| = V_m = \sqrt{(v_{qs}^s)^2 + (v_{ds}^s)^2} = \sqrt{(v_{qs}^2 + v_{ds}^2)} \quad (3)$$

The exponential factor is the VR (Vector Rotator Factor as such).

Additionally, a similar representation of the complex phasor  $V'$  is also specifically possible in terms of the original three phase components as follows:

Obviously similar transformations can also be performed on the rotor portion of the circuits.

The various expressions for flux linkages are as thus based on the above diagrams (Fig. 1.3):

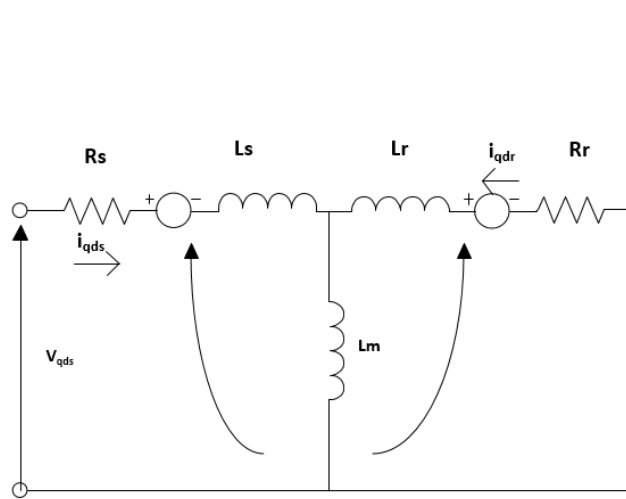
All the quantities appear here in these circuits as dc quantities due to the properties of the de-qe model. The final expressions of voltages in terms of currents using the flux linkages and representing them in term of the corresponding inductances are as follows:

$$\begin{bmatrix} v_{qs} \\ v_{ds} \\ v_{qr} \\ v_{dr} \end{bmatrix} = \frac{2}{3} \begin{bmatrix} R_s + SL_s & \omega_e L_s & SL_m & \omega_e L_m \\ -\omega_e L_s & R_s + SL_s & -\omega_e L_m & SL_m \\ SL_m & (\omega_e - \omega_r)L_m & R_r + SL_r & (\omega_e - \omega_r)L_r \\ -(\omega_e - \omega_r)L_m & SL_m & -(\omega_e - \omega_r)L_r & R_r + SL_r \end{bmatrix} \begin{bmatrix} i_{qs} \\ i_{ds} \\ i_{qr} \\ i_{dr} \end{bmatrix} \quad (4)$$

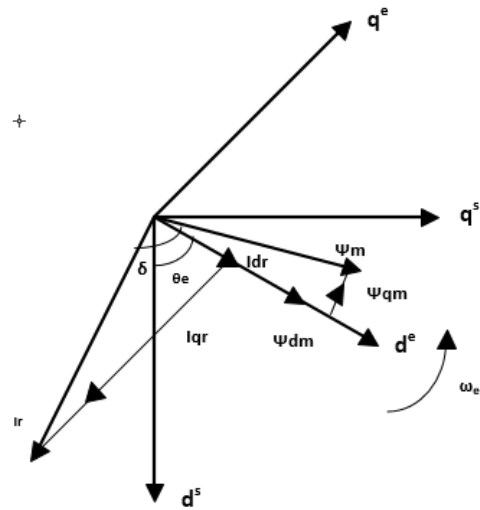
S is the Laplace differential operator d/dt.

Here if  $\omega_r$  is taken to be constant than the system is fourth order linear system.

For compact representation we can again obtain the space phasor approach by merging  $v_{qs}$  and  $v_{ds}$  together.



1.4 dq<sub>s</sub> equivalent circuit



F1.5 Current and Flux vectors in Induction Machine

This is the resulting complex representation of the circuit using the complex equations obtained for both the stator and rotor.

## **CHAPTER 3: Closed Loop Control of AFE in simultaneous operation**

- Conventional front-end converters are utilized for active power flow mainly between the load and the grid, while active filters consume energy to ensure a harmonic injection that suppresses all the line current harmonics generated due to the connection of non-linear loads.
- However quite often it is relatively costlier to equip both the PWM based front end converter and the active filter, in those situations we defer towards the utilizations of a PWM converter as a combination of both the individual elements in conjunction. However, such a combination needs for a clear definition of priority and internal compromises between the supply power flows, the regeneration power and the associated compensate powers. For this purpose, an adaptive gain control block is utilized.

### **3.1 Operation of the PWM Converter Simultaneously as Active Front end Converter and Active Filter.**

- The various equations relevant to this converter and its model are as follows:
- Here  $u_L$  represents the line voltage,  $u_i$  the drop between the interconnected supply and the converter and  $u_s$  the converter modulated voltage.

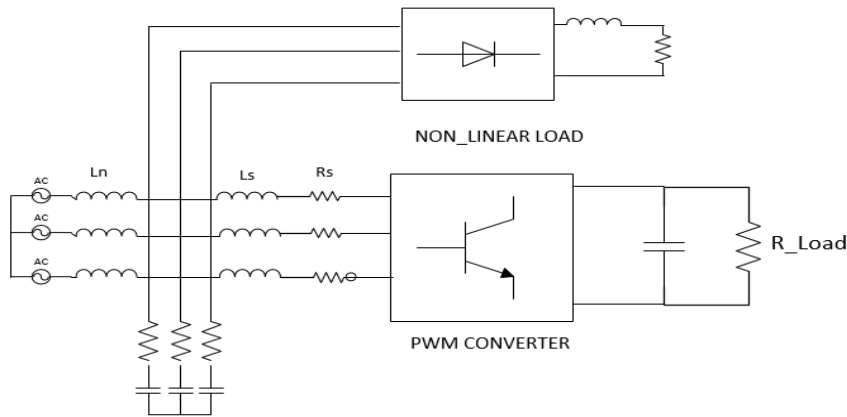


Fig 3.1 The Generic Front-End Converter with Non-Linear Load

Using KVL, and subsequently representing in a matrix format,

$$u_L = u_i + u_s \quad (1)$$

$$\text{And, } u_L = Ri_L + L \frac{di_L}{dt} + u_s \quad (2)$$



$$\text{Hence, } \begin{bmatrix} u_a \\ u_b \\ u_c \end{bmatrix} = R \begin{bmatrix} i_a \\ i_b \\ i_c \end{bmatrix} + L \frac{d}{dt} \begin{bmatrix} i_a \\ i_b \\ i_c \end{bmatrix} + \begin{bmatrix} u_{sa} \\ u_{sb} \\ u_{sc} \end{bmatrix} \quad (3)$$

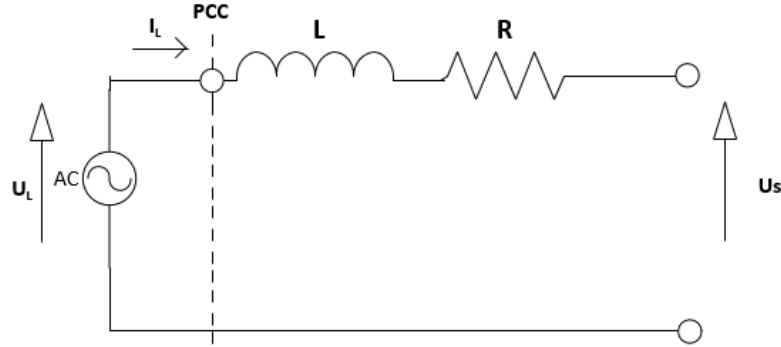


Fig 3.2 Simplified Model of the main load side of the Converter

### The Transform Equations:

- In the  $\alpha\beta$  and the  $dq$  rotating reference frame (rotating at speed corresponding to the supply frequency) we have the following equations as seen from Fig.3.2:

$$\begin{bmatrix} u_{L\alpha} \\ u_{L\beta} \end{bmatrix} = R \begin{bmatrix} i_{L\alpha} \\ i_{L\beta} \end{bmatrix} + L \frac{d}{dt} \begin{bmatrix} i_{L\alpha} \\ i_{L\beta} \end{bmatrix} \begin{bmatrix} u_{s\alpha} \\ u_{s\beta} \end{bmatrix} \quad (4)$$

This equation in the  $dq$  frame is obtained as follows:

$$u_{Ld} = Ri_{Ld} + L \frac{di_{Ld}}{dt} - \omega Li_{Lq} + u_{sd} \quad (5)$$

$$u_{Lq} = Ri_{Lq} + L \frac{di_{Lq}}{dt} - \omega Li_{Ld} + u_{sq} \quad (6)$$

- The PWM output  $u_s$  controls the power flow, i.e. as a rectifier or as an inverter.
- $u_s$  and its maximum value is dependent on the modulation scheme used as well as the dc voltage level.
- Magnitude and phase of  $u_s$  defines the power flow.

The inductance has the following importance:

- a. It deliberates the current source characteristics of the input. b. It also provides a boost of voltage.
- The line current is also controlled by the inductance voltage drop. Since the  $\varepsilon$  and  $u(s)$  of the source are controllable via the modulation scheme, for a given line voltage, we have a situation whereby the phase and the amplitude of the line current is controllable indirectly. Additionally, as this voltage is controlled by the dc link voltage and current, the same quantities determine the active power requirements and active power flow from the converter to the source and vice versa.

### 3.2 Instantaneous Power Theory (p-q theory)

- The p-q theory is utilized for the power control of Shunt Active Filter, as well in cases where simultaneous operation is taken into consideration. Normally, an AFE is controlled by Vector Control of Voltage Vectors in dq reference frame and, but here we are utilizing the Hysteresis control methods which require reference currents, hence p-q theory is used.
- The various transforms and equations are as shown below:

$$\begin{bmatrix} u_\alpha \\ u_\beta \end{bmatrix} = \sqrt{\frac{2}{3}} \begin{bmatrix} 1 & -\frac{1}{2} & -\frac{1}{2} \\ 0 & \frac{\sqrt{3}}{2} & -\frac{\sqrt{3}}{2} \end{bmatrix} \begin{bmatrix} u_a \\ u_b \\ u_c \end{bmatrix} \quad (1)$$

$$So, \begin{bmatrix} i_\alpha \\ i_\beta \end{bmatrix} = \sqrt{\frac{2}{3}} \begin{bmatrix} 1 & -\frac{1}{2} & -\frac{1}{2} \\ 0 & \frac{\sqrt{3}}{2} & -\frac{\sqrt{3}}{2} \end{bmatrix} \begin{bmatrix} i_a \\ i_b \\ i_c \end{bmatrix} \quad (2)$$

- The powers in the  $\alpha\beta$  reference frame is obtained as follows:

$$\begin{bmatrix} p \\ q \end{bmatrix} = \begin{bmatrix} u_\alpha & u_\beta \\ -u_\beta & u_\alpha \end{bmatrix} \begin{bmatrix} i_\alpha \\ i_\beta \end{bmatrix} \quad (3)$$

$$\text{Taking inverse, we get } \begin{bmatrix} i_\alpha^* \\ i_\beta^* \end{bmatrix} = \frac{1}{u_\alpha^2 + u_\beta^2} \begin{bmatrix} u_\alpha & u_\beta \\ u_\beta & -u_\alpha \end{bmatrix} \begin{bmatrix} p \\ q \end{bmatrix} \quad (4)$$

- These are the equations for the compensator current. The p and q invariant powers are powers absorbed by the compensator.[2]

### 3.3 Power Flow Control Strategy

- Here p & q are controlled independently.
- These powers are respectively controlled via references related to the DC-load power and the compensating power. A conventional PWM converter, which exchanges purely active power for unity power factor control.
- In the case of an active filter however, the commands of p and q depend on the compensated load as such. With the supply assumed constant they are directly controlled via the active and reactive current components.
- Controlling the active power flow is in fact controlling the dc voltage of the capacitor. If the capacitor voltage is above set reference, it works as an inverter otherwise when capacitor voltage is lower than reference, as a rectifier.

- Using a PI controller as a dc voltage regulator, we can utilize its output to deliver the active power command to the inner current controller as the power flows are in fact controlled of the grid via the currents.
- Additionally, a non-linear load has a tendency to draw an additional oscillating power component over and above the average power value. This oscillating power component is also to be compensated in the grid lines. Thus, we have the reactive power compensation along with the oscillating power compensation needed by the converter. (Refer Fig. 3.3)
- This power also usually does not tend to be utilitarian, rather one that contributes in the losses of the system along with the heating.  $\mathbf{p} = \mathbf{p}_{avg} + \mathbf{p}_{oscillatory}$ . We can extract the oscillating component for its compensation by using a low pass filter that allows the average component of power to pass through as is. This generates the compensation command of the active power. The control schematic is shown in the subsequently. [8]

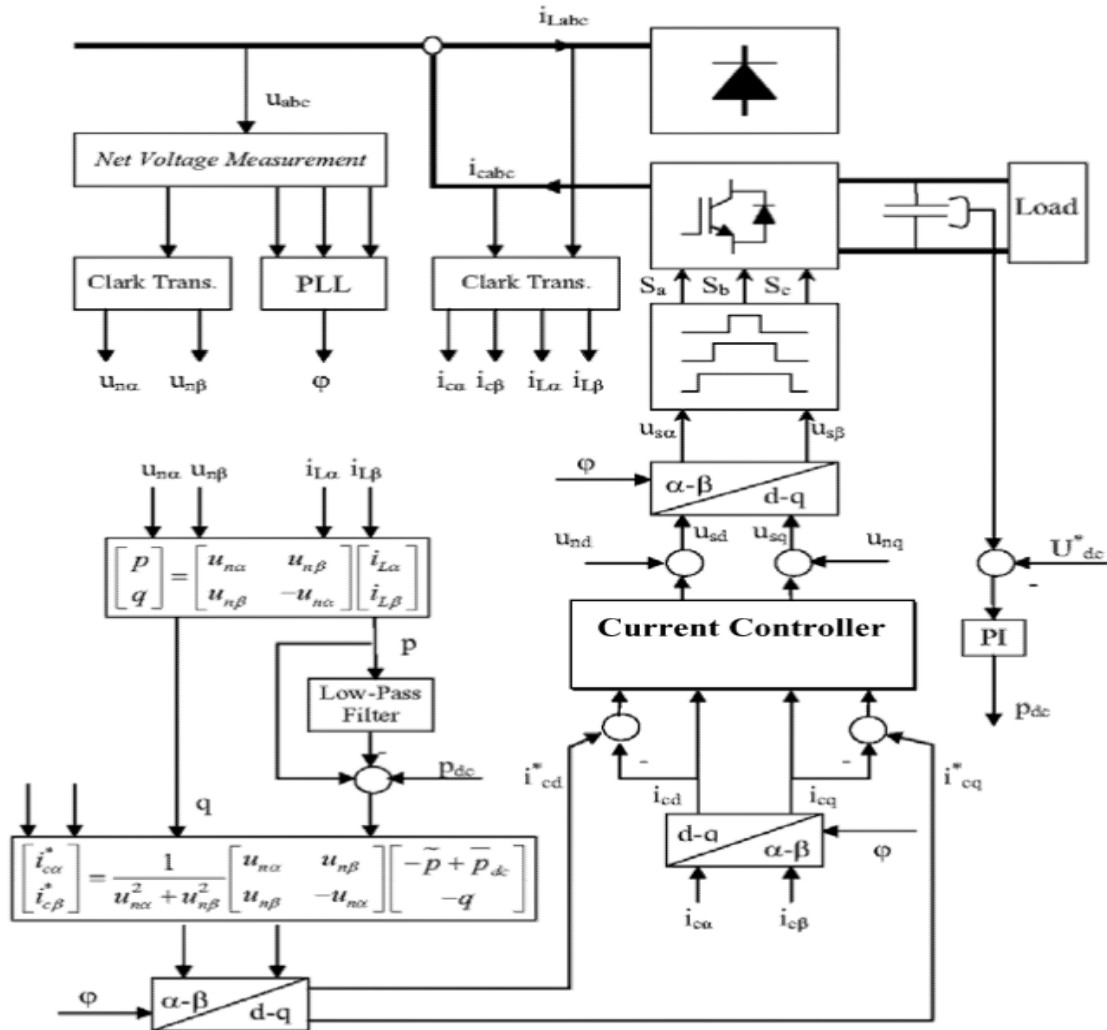


Fig 3.3 Overall schematic of Control Scheme

- Here the Active Component absorbed:  $p_{(dc\ link)} - p_{(oscillatory)}$  The oscillatory component is generated by the converter to supply the non-linear load. Additionally, we have a situation whereby the dc link power is absorbed by the compensator. Similarly, the reactive power is also supplied by it  $(-q)$  for compensation. These compensator reference currents are then converted to their dq frame, and via the sensed compensator currents the error is mitigated. Additionally, the compensator currents along with the compensator network parameters defines using the supply volts the compensator volts using the equations of the dq transform so obtained.
- After transforming into  $\alpha\beta$  the switching signals are then sent to the inverter legs. Here line voltage is measured and transformed. A PLL generates the speed utilized for the Park Transform Block. (Refer Fig. 2.4) The voltages are converted to their stationary reference frame currents via the Clarke transform. Additionally, the line and the compensator currents are also sensed and transformed. All quantities are converted to their Clarke Transform form. Based on the line voltage and current so sensed, we obtain the instantaneous powers in line with the p-q block theory.
- A low pass filter extracts the oscillatory component from this value of p so obtained, which is then added with the dc link power that the converter needs. Thus, based on the reactive power sensed the currents generated are such that the compensator absorbs the following powers: The capacitor voltage is sensed and compared with the reference for the generation of the active power command. This error signal, when given to PI generated the  $p_{dc}$  signal. Fig. 3.4 shows clearly the Control scheme block diagram.

### 3.4 The Adaptive Gain Control scheme

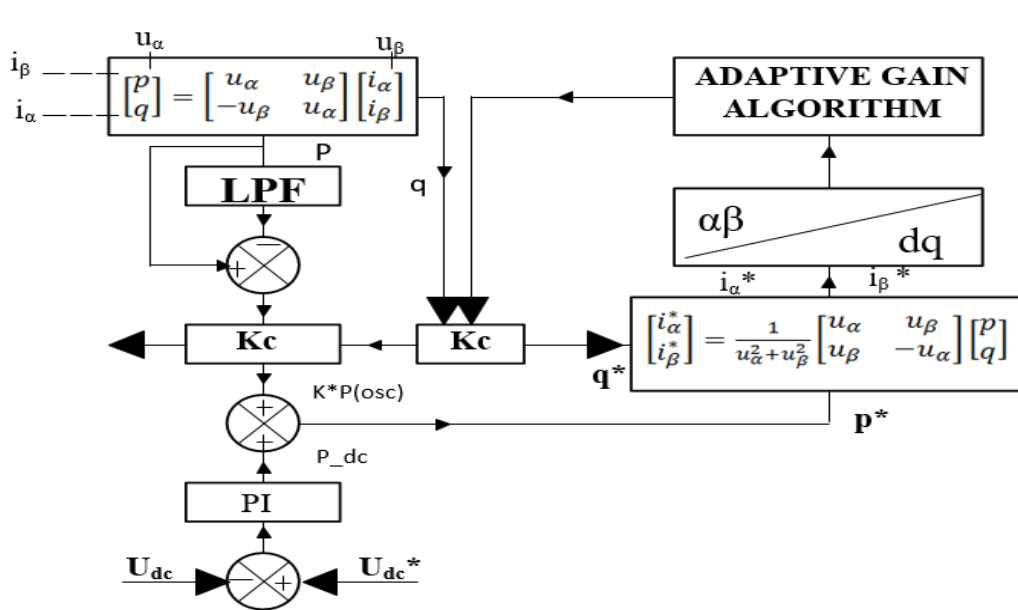


Fig 3.4 Adaptive Control of Gain

- Obviously, each converter has its own power rating based on the maximum current that the IGBT switches and other semiconductor elements can withstand. Thus, based on such a limit of current and the power flow corresponding to this current, we give the active power flow compensation and the dc link power flow the first priority.
- The reactive power compensation is given the second priority is between 0 and 1.
- Once the active power criteria are matched the reactive compensation is done up until the maximum power/current limit of the switches is reached.
- Subsequently the following algorithm is utilized for these purposes in conjunction with the  $K_c$  value obtained/determined. The algorithm for finding  $K_c$  has been shown in Fig.3.5 [2]

### Adaptive Control Algorithm

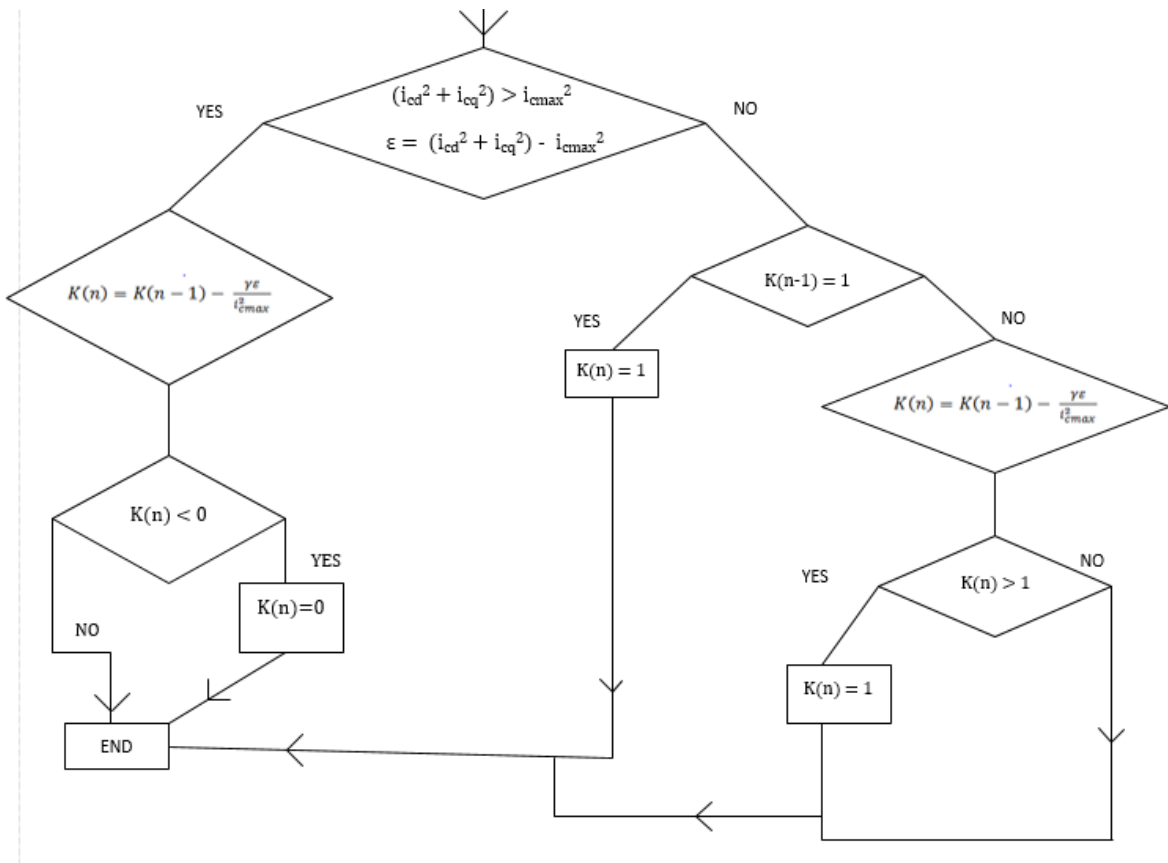


Fig 3.5 Algorithm

- Here  $\lambda$  is a positive constant dependent on the modifications in  $K_c$  permitted.

- Thus, this adaptive algorithm allows the compensator to work also as a shunt filter by injecting required oscillating active power needed by the non-linear load and also by reactive power compensation of the load reactive power.

### 3.5 Compensating Reference Current Generation

The compensating reference currents are generated by implementing the p-q instantaneous power theory as per the Overall schematic shown. The total power consumed is hence subtracted from the average power consumption to get the oscillatory component of power. Then, the compensating reference currents are generated in the 2-phase stationary frame of reference – alpha-beta frame. These reference currents are then converted to 3 phase abc reference frame to get the respective reference currents. The first part of our circuit is now completed. These reference currents will be in further compared with measured actual currents to get the desired current control.

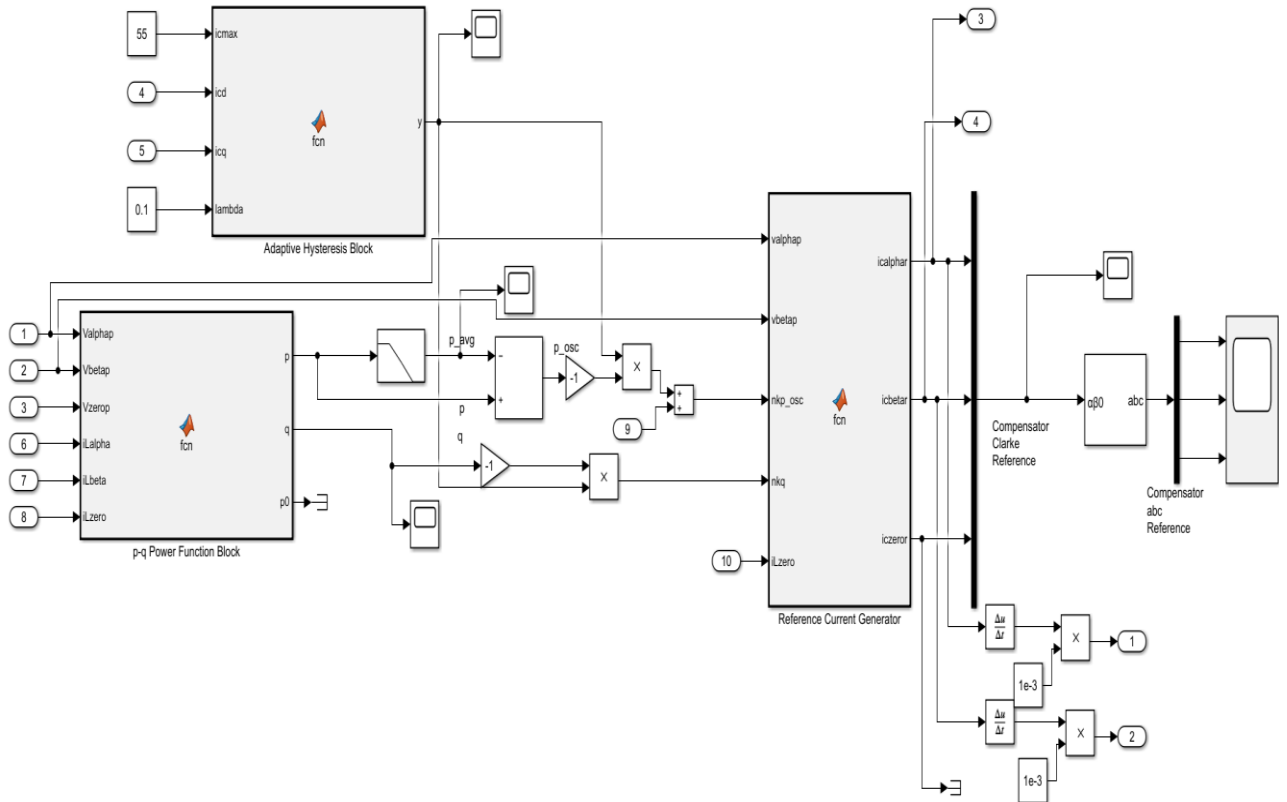


Fig.3.6 Reference current generation Block

## CHAPTER 4: Current Control Strategies

The applications involving the control of Voltage Source based Pulse Width Modulated Converters have a close loop control structure having a current feedback loop. Hence, the quality of converter system largely depends on the performance of applied current control strategy.

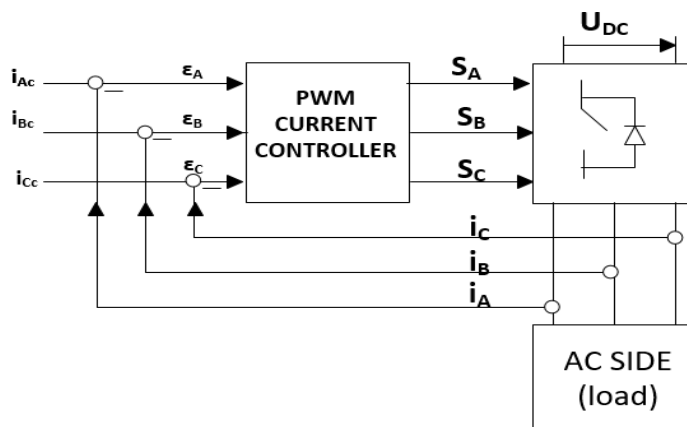


Fig. 4.1 Block diagram of current controlled PWM converter

The basic principle is that the modulation process controls the phase switching sequence according to a given reference so that phase voltage along low order harmonics result in a waveform which follows the reference as closely as possible.

### 4.1 Advantages of current- controlled PWM converters:

- 1) control of instantaneous current waveform and better accuracy;
- 2) control and protection from peak currents and rejection of overload currents;
- 3) better circuit dynamics;
- 4) compensation to effects of load parameter changes;
- 5) compensation of voltage drops across semiconductors and dead-time of converters;
- 6) compensation of dc link voltages as well as ac-side voltage changes;

**Effect of current ripple:** Vector sequences with same resultant give equal mean voltages and therefore equal average currents, however it is important to note that different vector orientations give different current ripples. A sensible ripple reduction is obtained when the phase pulses are centered and symmetrical in nature.

**Effect of phase voltages:** While the phase voltages are controlled independently, the phase currents are determined by the phase voltages of not only their own phase but also the other phases. This phase interference has to be taken into account while designing the current controller.

## 4.2 HYSTERESIS – DELTA CURRENT Controller

The major classes of controllers developed till date are:

1. Linear PI regulators
2. Hysteresis regulators
3. Predictive dead-beat regulators

Among all these, the hysteresis regulator is implemented very often because of its simplicity, fast current response and lack of necessity to know about the load parameters. The only visible disadvantage of this method is that the Pulse Width Modulated frequency varies within a band because the peak to peak current ripple has to be controlled at all points of the fundamental frequency wave.

The implementation is as follows:

The delta modulation or current error is calculated as the difference between actual currents and reference currents, which is then compared to a fixed tolerance band. This type of band control gets affected negatively by interaction of different phase currents, which is a typical behavior in three phase systems.

This happens because of the interference between the commutations of the three phases. Each phase current not only depends on the corresponding phase voltage, but also gets affected by the voltage of the other two phases. Depending on load parameters, the switching frequency may vary during the fundamental period which results in irregular inverter operation.

The band is constant, and the current keeps on rising until it reaches the upper limit, after which it continues to fall unless met by the lower limit. This has been shown in the Fig. 4.3. Note, the only difference between the 3-phases is in their angular phase and the width of the band remains constant.

A new method has been proposed that minimizes the effect of interference between phases while maintaining the advantages of the hysteresis methods by using phase-locked loop (PLL) technique to constrain the inverter switching at a fixed predetermined frequency. [9]

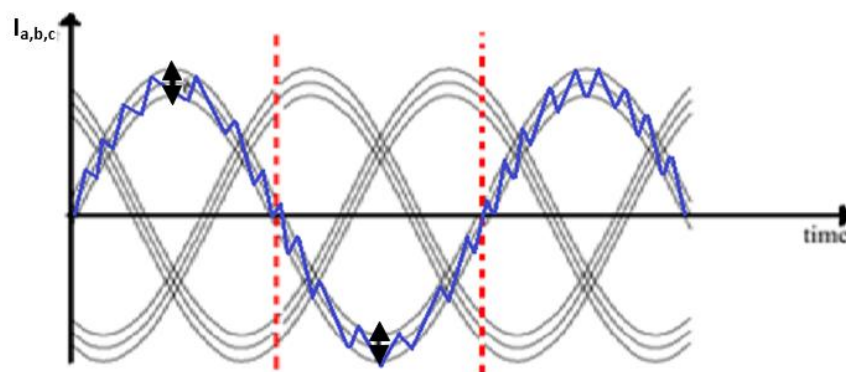


Fig. 4.3 Hysteresis bands for three phase reference currents



The actual value of current has to be kept within the bands specified by the hysteresis algorithm. The currents being independent, are transformed into the  $(\alpha, \beta)$  co-ordinate system.

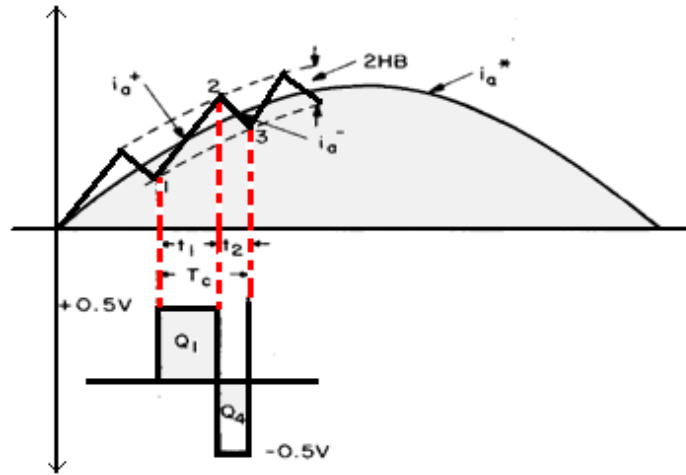


Fig: 4.4.1 Switching when upper and lower hysteresis band is reached.

A hysteresis-band current control method is used because of its simple to implement feature and dedicated hardware, fast response time, also the device peak current gets limited automatically. Performance (in terms of sharpness of line current) of the conventional controller is governed by the hysteresis band of the current error. With large value of hysteresis band, the switching frequency reduces correspondingly, but at the same time line current has more ripple, which results in a poorer waveform.

### 4.3 Disadvantages of Conventional Hysteresis Regulator:

- 1) The switching frequency of the converter is not constant, it keeps varying in a band, and hence depending on the values of load parameters. It also varies with ac voltage.
- 2) The rough operation of the regulator makes it difficult to protect the converter.
- 3) Limit cycle oscillations, overshoot in current error, generation of subharmonics in the input current, and random switching of voltage vectors are some of the major drawbacks of this technique.

In case of systems not having a neutral wire, the instantaneous errors can become twice of that of the hysteresis band value. Here, the system interacts with three independent controllers. There is a coupling present in between the phases, due to which change in one phase influences the voltage applied to the other two phases. If all three phase current errors are to be considered as space vectors, the interaction effect can be nullified, and many variants of controllers known as space-vector based can be created.

## 4.4 ADAPTIVE HYSTERESIS BAND BASED CONTROLLER

The general fixed hysteresis-band current controller generates much more current ripple because its modulation frequency varies within a predefined band. In adaptive hysteresis-band method, the band is modulated as a function of system parameters to maintain the modulation frequency to be nearly same. Systematic mathematical analysis has been presented, and band expressions have been derived as a function of the load machine and supply parameters.

The PWM Inverters usually utilized may either be controlled using scalar techniques or vector techniques. Usually systems which don't require tremendously fast dynamic response, and systems which usually work under steady state conditions, don't as such require any form of novel control technique excluding and more advanced than scalar techniques, and thus may utilize the same, however in circuits requiring quick dynamic response and fast performance, it is of utmost importance to utilize novel and extremely stable under dynamic conditions controllers, based on theories of vector control with appropriate inner and outer control loops.

Additionally, as the battery voltage increases there is a tendency of the switching frequency of the inverter increases which results in the upper switching frequency limit of the associated switches being violated. This thus results in a situation whereby the circuit, and the inverter is operating under extremely high frequency close to the limiting value of the inverters frequency limits. This again increases the switching losses of the inverter along with inhibiting the optimal performance of the inverter circuit. Thus, as the battery voltage usually ripples about its reference value, during transience, rather than set the value of the input dc-link voltage to the adaptive band calculating circuit as the actual voltage value, it is more optimal to set it at its worst-case value of reference assumed steady state value.

In line with the above discussion as the hysteresis band stays constant, the following problem occurs: due to constant band width, when the current excursions are terribly large switching of the switches is done at higher frequency and vice versa, giving us a large variation in switching frequency along with higher operating frequency and higher power loss, thus in order to restrict this particular current excursion the hysteresis band can be varied appropriately to ensure that when the current excursion are large, the hysteresis band is increased to reduce switching frequency and vice versa.

$$L \frac{di_a^+}{dt} = 0.5 Vb \text{ and } L \frac{di_a^-}{dt} = -0.5 Vb \quad (1)$$

$$\text{Hence, we can write by combining } \frac{di_a^+}{dt} + \frac{di_a^-}{dt} = 0 \quad (2)$$

where  $L$  = phase inductance, and  $i$ , + and  $i$ , - are rising and falling current segments respectively. From geometry, we can write

$$\frac{di_a^+}{dt} t_1 - \frac{di_a^*}{dt} t_1 = 2HB \text{ and} \quad (3)$$

$$\frac{di_a^-}{dt} t_2 - \frac{di_a^*}{dt} t_2 = -2HB \quad (4)$$

$$\text{Also, } t_1 + t_2 = T_c = \frac{1}{f_c} \quad (5)$$

where  $t_1$  and  $t_2$  are the respective switching intervals, and  $f_c$  is the frequency of modulation. Adding above equations, we can write

$$t_1 \frac{di_a^+}{dt} + t_2 \frac{di_a^*}{dt} - \frac{1}{f_c} \frac{di_a^*}{dt} = 0 \quad (6)$$

$$4HB = t_1 \frac{di_a^+}{dt} - t_2 \frac{di_a^-}{dt} - (t_1 - t_2) \frac{di_a^*}{dt} \quad (7)$$

$$4HB = (t_1 + t_2) \frac{di_a^+}{dt} - (t_1 - t_2) \frac{di_a^*}{dt} \quad (8)$$

$$= \frac{1}{f_c} \frac{di_a^+}{dt} - (t_1 - t_2) \frac{di_a^*}{dt} \quad (9)$$

$$\text{Therefore, we can write } t_1 - t_2 = \frac{\frac{di_a^+}{dt}}{\left(\frac{di_a^*}{dt}\right)} \quad (10)$$

$$4HB = \frac{1}{f_c} \left[ \frac{di_a^+}{dt} - \frac{\left(\frac{di_a^*}{dt}\right)^2}{\left(\frac{di_a^+}{dt}\right)} \right] \quad (11)$$

$$\text{Thus, } HB = \frac{0.125V_b}{f_c L} \left[ 1 - 4 \frac{m^2 L^2}{V_b^2} \right] \quad \dots \text{Final Equation} \quad (12)$$

$$\text{Hence, } f_c = \frac{0.125V_b}{(HB)L} \left[ 1 - 4 \frac{m^2 L^2}{V_b^2} \right] \quad (13)$$

Eqn. (12) shows the hysteresis band as a function of modulation frequency, supply voltage, and the slope of the  $i_a$  wave. Eqn. (13) indicates that for a fixed band, the modulation frequency will vary with  $V_b$ , shows the sensitivity of  $f_c$  with  $V_b$ , indicating that the modulation frequency increases with the dc voltage.

The slope  $m$  varies as:

$$m^2 = \left[ \frac{d}{dt} (I_m \sin \omega t) \right] = 0.5 \omega^2 I_m^2 (1 + \cos 2 \omega t) \quad (14)$$

The line to neutral voltages, can be written as

$$v_{an} = \frac{2}{3} v_{a0} - \frac{1}{3} (v_{b0} + v_{c0}) \quad (15)$$

$$v_{bn} = \frac{2}{3} v_{b0} - \frac{1}{3} (v_{a0} + v_{c0}) \quad (16)$$

$$v_{cn} = \frac{2}{3} v_{c0} - \frac{1}{3} (v_{b0} + v_{a0}) \quad (17)$$

$$\Delta HB = \frac{t_{1n}}{L} (a v_b - v_f) + t_{1n} m \quad (18)$$

Where the possible values of  $a = 0, \frac{1}{3}$  or  $\frac{2}{3}$  and  $m = \frac{di_a^*}{dt}$  (slope) (19)

$$2HB = \Sigma \Delta HB = \Sigma \left[ -t_{1n} \left( m + \frac{v_f}{L} \right) + \frac{1}{L} * t_{1n} * V_b \right]$$

$$= -t_1 \left( m + \frac{v_f}{L} \right) + \frac{1}{L} \Sigma t_{1n} * a * V_b \quad (20)$$

The general expression for the current fall is given as:

$$-\Delta HB = \frac{t_{2n}}{L(aV_b + v_f)} - t_{2n} * m \quad (21)$$

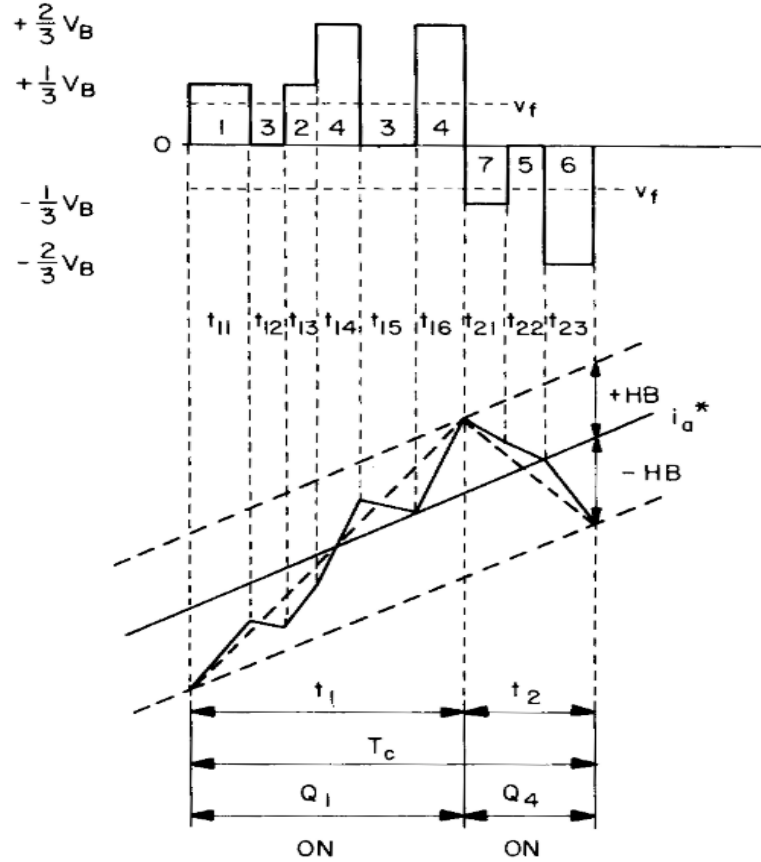


Fig 4.4.2 PWM phase voltage and current waves for a modulation cycle in isolated neutral wave

$$-\Delta HB = \frac{t_{2n}}{L} (aV_b + v_f) - t_{2n} m \quad (22)$$

The above eqn. (22) gives the general expression of the current fall

Therefore the total fall is,

$$-2HB = \Sigma \left[ -t_{2n} \left( m + \frac{v_f}{L} \right) - \frac{1}{L} t_{2n} * a * V_b \right] \quad (23)$$

$$= -t_2 \left( m + \frac{v_f}{L} \right) - \frac{1}{L} \Sigma t_{2n} * a * V_b \quad (24)$$

The rise and fall of currents the periods  $t_1$  and  $t_2$  respectively, are shown in Fig. 4.4.2 The slope of these lines can be determined by the weighted average of supply voltage.

$$\Sigma t_{1n} * a * Vb = t_1 * a' * Vb \quad (25)$$

$$\Sigma t_{2n} * a * Vb = t_2 * a' * Vb \quad (26)$$

$$\text{Hence, } a' = \frac{\Sigma t_{1n}}{t_1} \text{ and } a'' = \frac{\Sigma t_{2n}}{t_2} \quad (27)$$

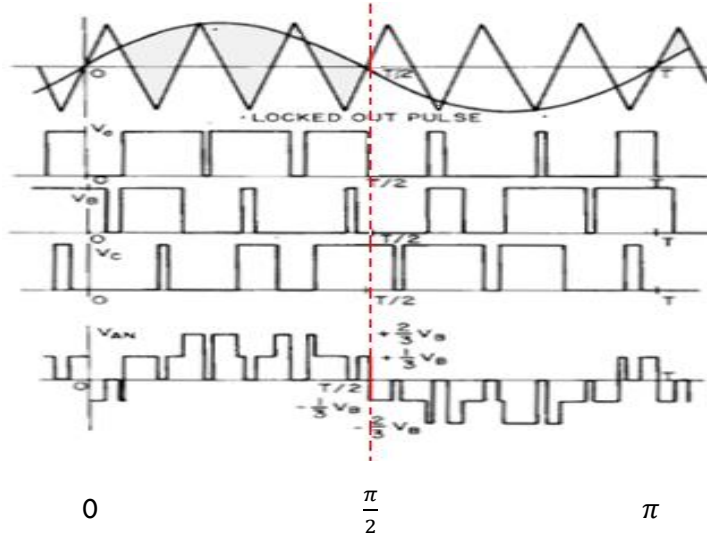


Fig 4.4.2 Typical PWM voltage waves when thr machine neutral is isolated

where  $a'$  and  $a''$  are the coefficients representing applied voltages respectively. The average value of applied voltages in two intervals have some degree of asymmetry, it's assumed that they are same (i.e.,  $a' = a''$ ) for reduction in the amount of computational complexity. The computation of HB on this hypothesis gives a result with greater accuracy. The parameters  $a$ ,  $a'$ , and  $a''$  must stay between  $1/3$  to  $2/3$ , where latter is the worst possible outcome. Combining the equations, we get

$$HB = \frac{0.25 * a' * Vb}{f_c L} \left[ 1 - \frac{L^2}{a'^2 Vb^2} \left( \frac{vf}{L} + m \right) \right] \quad (28)$$

The final equation obtained on deriving to the conditions of our case is implemented in MATLAB function block, which happens to be slightly different as compared to eqn. (28) and eqn. (12) This is on account of the difference in topology of the circuit implemented, which has been shown in Fig. 5.5. However, there are just few more terms due to load emf and the line inductance, and the empirical formula remains almost the same.

## 4.5 CURRENT ERROR SPACE PHASOR BASED HEXAGONAL HYSTERESIS CONTROL

### 4.5.1 Introduction

The results obtained with an adaptive hysteresis controller aren't as satisfactory as one would predict. The objective of producing sinusoidal ac input currents is totally dependent on the current control technique employed, particularly in case of current regulated PWM converters. The major task which a controller carries out is that of forcing of the current vector according to the reference generated.

The adaptive band is supposed to have superior output compared to normal hysteresis band, however not much difference in harmonic spectrum is observed due to the interaction of phase currents. The phase currents depend on voltages of not only the corresponding phases, but also on the voltages of the adjacent phases – due to this, the harmonics still persist in the system. The effect of these phase interactions can be eliminated by introducing a PLL into the circuit, which mathematically changes the generation of adaptive band parameter such that the effect of the other phase voltages is nullified. [9]

The proposed method is implemented in stationary reference frame ( $\alpha, \beta$  frame), wherein the three phase hysteresis bands are converted into a hysteresis hexagon. [10]

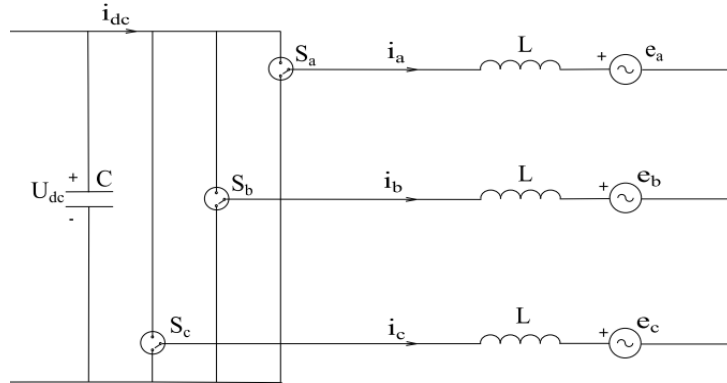


Fig 4.5: Power Circuit Topology

The method is based on simple Space Vector Modulation Strategy, for a two level three phase VSI, which has been accordingly modified to accommodate the changes that will be encountered for a converted based circuit. The inverter operation is possible in 8 modes of switching ( $2^3=8$ ), wherein 6 voltage states are active states and the rest two are passive ( $S_a, S_b, S_c = 0,0,0$  or  $1,1,1$ ).

On transforming from three-phase (a, b, c) into stationary ( $\alpha, \beta$ ) coordinate system:

$$\begin{bmatrix} u_\alpha \\ u_\beta \end{bmatrix} = \begin{bmatrix} \frac{2}{3} & -\frac{1}{3} & -\frac{1}{3} \\ 0 & \frac{\sqrt{3}}{2} & -\frac{\sqrt{3}}{2} \end{bmatrix} \begin{bmatrix} u_a \\ u_b \\ u_c \end{bmatrix} \quad (1)$$

The equation (1) is not written in a power invariant fashion, rather in a power variant fashion.

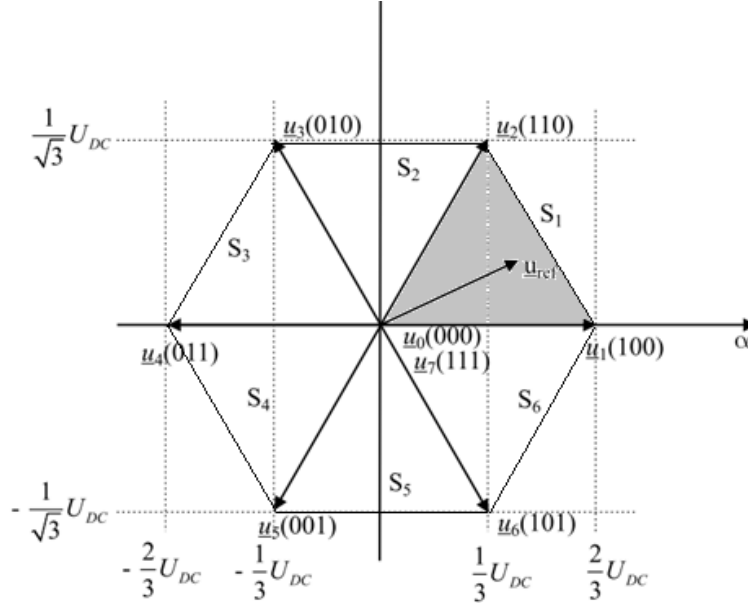


Fig.4.6 Switching states of VSI output voltages. Reference voltage present in sector  $S_1$ .

State	$S_a$	$S_b$	$S_c$	$u_a/U_{dc}$	$u_b/U_{dc}$	$u_c/U_{dc}$	$u_{ab}$	$u_{bc}$	$u_{ca}$	$u_a/U_{dc}$	$u_\beta/U_{dc}$
$u_0$	0	0	0	0	0	0	0	0	0	0	0
$u_5$	0	0	1	-1/3	-1/3	2/3	0	-1	1/3	-1/3	$-1/\sqrt{3}$
$u_3$	0	1	0	-1/3	2/3	-1/3	-1	1	0	-1/3	$1/\sqrt{3}$
$u_4$	0	1	1	-2/3	1/3	1/3	-1	0	1	-2/3	0
$u_1$	1	0	0	2/3	-1/3	-1/3	1	0	-1	2/3	0
$u_6$	1	0	1	1/3	-2/3	1/3	1	-1	0	1/3	$-1/\sqrt{3}$
$u_2$	1	1	0	1/3	1/3	-2/3	1	1	-1	1/3	$1/\sqrt{3}$
$u_7$	1	1	1	0	0	0	0	0	0	0	0

Table:1 On/Off output states of three-phase VSI.

#### 4.5.2 Principle of Hexagon Hysteresis Control:

In normal hysteresis type control, the goal is to keep the currents within the hysteresis bands at all the times. Similarly, in case of hexagonal hysteresis, the idea is to keep the current error space phasor within the hexagon at all times

The hexagon represents the hysteresis bands within which the current error phasor ( $i_e$ ) is supposed to vary. It is note-worthy to understand that the hexagon boundaries' dimensions are fixed (corresponding to a fixed hysteresis band) however, the idea is to keep the error between the actual and reference current to a minimum. Hence as the reference current is not constant, but rather keeps rotating in the  $\alpha$ - $\beta$  reference frame, so does the hysteresis hexagon. It is a constant magnitude revolving hexagon. [10]

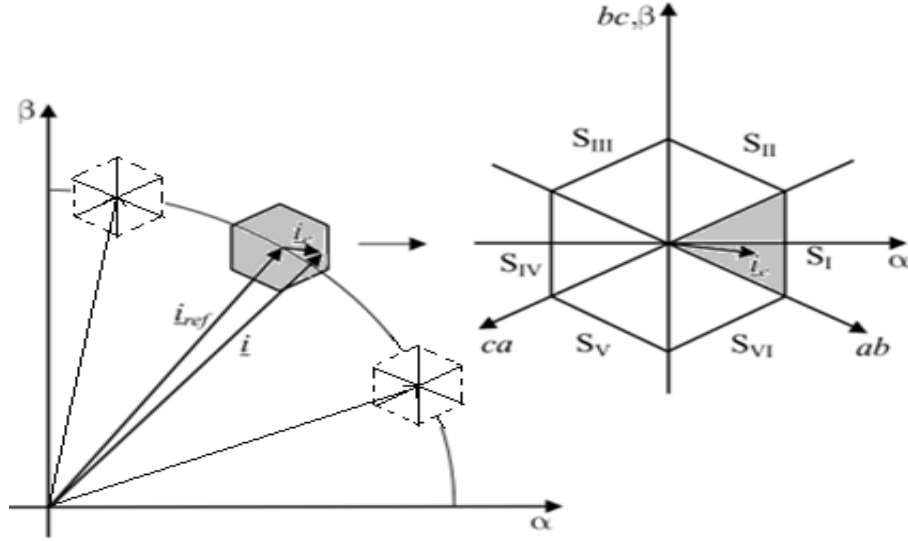


Fig.4.7 Hysteresis Hexagon in  $(\alpha, \beta)$  plane. Current error phasor is present in sector  $S_I$ . The reference current rotates, and so does the hysteresis hexagon, but the reference current always points at the centre of the hexagon.

#### 4.5.3 Structure of hysteresis control:

The current error phasor ought to remain inside the hysteresis hexagon at all times. When the phasor touches the boundary of the hexagon, the idea is to trigger a voltage vector such that the current error phasor is forced inside the boundary of the hexagon.

The current error, is the difference between actual current and reference current:  $\mathbf{i}_e = \mathbf{i} - \mathbf{i}_{ref}$  (2)

Now a regular hysteresis band would be controlled by the comparison between the measured and reference currents of each phases and hence generating the gating pulses.

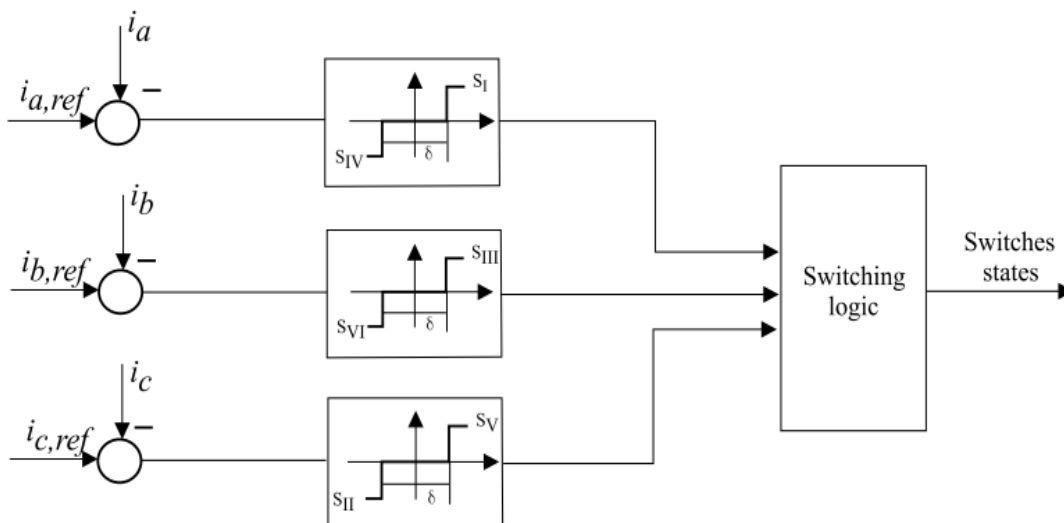


Fig.4.8 General Schematic of Hysteresis Control.



#### 4.5.4 Principle adopted for Switching Sequence Generation

The logic chosen for generating the switching pulses is quite simple:

- 1) If the current error phasor touches the boundary of hexagon, it has to be made to reach the centre of the hexagon as slowly as possible in order to have the most optimized switching rates – to ensure low value of switching frequency.
- 2) If the current error phasor tip is already outside the boundary of the defining hexagon, in that case the phasor is made to reach the centre as soon as possible. This is in order to account for transient conditions.

$$\frac{di}{dt} = \frac{1}{L}(u_k - e) \quad (3)$$

$$\frac{die}{dt} = \frac{di}{dt} - \frac{di_{ref}}{dt} \quad (4)$$

$$\frac{die}{dt} = \frac{1}{L}(u_k - u_{ref}) \quad (5)$$

where the reference voltage is defined by,

$$u_{ref} = e + \frac{L di_{ref}}{dt} \quad (6)$$

This reference voltage is the one that ensure that the actual current and reference currents are identical.

In order to determine the most optimal of the eight switching states, we need two important parameters:

- 1) The Sectors  $S_I, S_2, S_3, \dots$  of the reference voltage according to the fig.
- 2) The Sectors  $S_I, S_{II}, S_{III} \dots$  Of the current error phasor according to the fig.

Case 1: Let's consider a particular sector, say Sector 1:

If  $i_e$  touches the boundary of sector  $S_I$ , then according to our principle, it has to brought back as slowly as possible to the center of the hexagon, therefore  $i_e$  must move in direction of negative  $\alpha$ -component. This requires the vector  $u_k - u_{ref}$  to have a negative  $\alpha$ -component. The hatched areas  $A_0, A_3, A_4$  and  $A_5$  corresponding to voltage vectors  $u_0, u_3, u_4$  and  $u_5$  are possible to trigger.

Now, according to equation (5), the the rate of change in current error phasor is directly proportional to length of vector  $u_k - u_{ref}$ . Hence, in order for the switching frequency to be as low as possible, the length of the vector from the Sector  $S_I$  has to be minimum, meaning that the length of the vector should the smallest. Here,  $u_0$  would be the vector of optimal choice. Note that the length of the vector is seen from the  $bc$  axis (which now, is perpendicular to the outer boundary of the sector  $S_I$ ) as shown in figure 4.19.

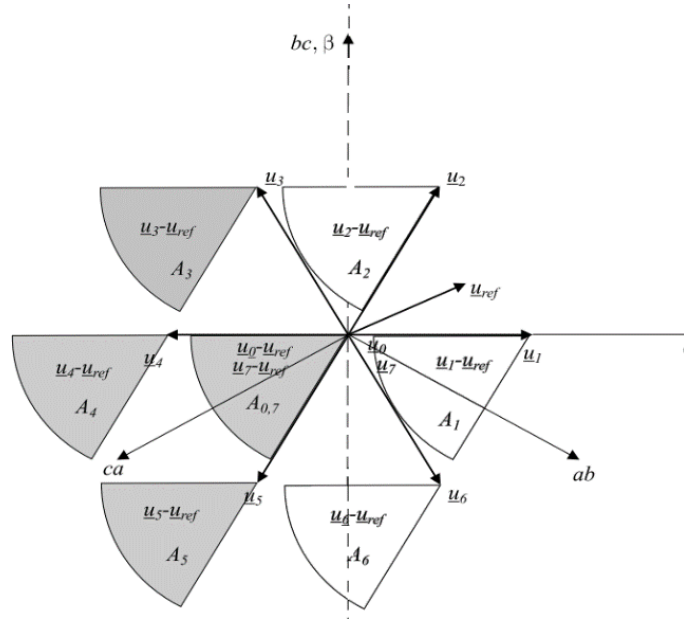


Fig.4.9 Hatched areas  $A_0$ ,  $A_3$ ,  $A_4$  and  $A_5$  and  $bc$ -axis shown.

Similarly, if the current error phasor were to be in sector  $S_{II}$ , the axis of reference from which the distance of the vector  $u_k - u_{ref}$  were to be determined would have been  $ab$  axis. ( $ab$  now being the axis perpendicular to the boundary of Sector  $S_{II}$ . Hence, hatched areas  $A_0$ ,  $A_4$ ,  $A_5$  and  $A_6$  (here corresponding to vectors  $u_0$ ,  $u_4$ ,  $u_5$ ,  $u_6$ ) are the ones which might be triggered after going through the second condition. The hatched areas are highlighted in the fig. 4.10 as shown below.

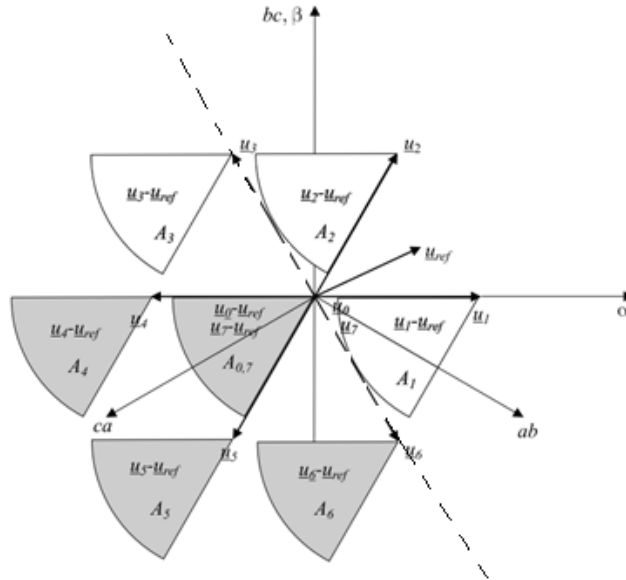


Fig.4.10 Hatched areas  $A_0$ ,  $A_4$ ,  $A_5$  and  $A_6$  and  $ab$ -axis shown.

Based on the same principle the voltage vectors corresponding to the presence of the current error phasor in all six sectors are determined in order to form a complete switching table.

#### 4.5.5 Switching Table

Sectors	$S_I$	$S_{II}$	$S_{III}$	$S_{IV}$	$S_V$	$S_{VI}$
$S_1$	$u_{0,7}$	$u_{0,7}$	$u_1$	$u_1$	$u_2$	$u_2$
$S_2$	$u_3$	$u_{0,7}$	$u_{0,7}$	$u_2$	$u_2$	$u_3$
$S_3$	$u_4$	$u_4$	$u_{0,7}$	$u_{0,7}$	$u_3$	$u_3$
$S_4$	$u_4$	$u_5$	$u_5$	$u_{0,7}$	$u_{0,7}$	$u_4$
$S_5$	$u_5$	$u_5$	$u_6$	$u_6$	$u_{0,7}$	$u_{0,7}$
$S_6$	$u_{0,7}$	$u_6$	$u_6$	$u_1$	$u_1$	$u_{0,7}$

Table:2 Switching Table for Hexagonal Band Hysteresis controller.

The above switching table incorporates only those cases wherein the switching frequency is supposed to be low, i.e. cases wherein the boundary of the hexagon is not crossed by the tip of the current error phasor. In case it does, which indicates a dynamic change has occurred, then the current error phasor will be perhaps lying way outside the hysteresis hexagon and we need to push it back inside as soon as possible. This is done by setting another hexagon shaped hysteresis boundary outside our regular hexagon, which corresponds to the dynamic hysteresis boundary.

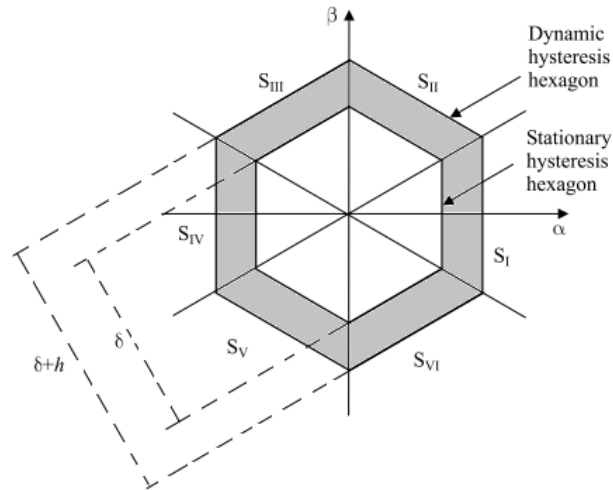


Fig. 4.11 Stationary and Dynamic Hysteresis Hexagon.

When the current error lies in the shaded region, meaning a fast change in current error is expected, the switching pattern is decided based on the direction of the current error phasor and the sector of the reference voltage vector is of no use. The sector lying exactly opposite to the sector of  $i_e$  needs to be triggered.

For e.g. if the current error vector lies in sector  $S_I$ , in order to bring it back to the stationary limits as soon as possible, the voltage vector  $u_4$  is to be triggered.

Sector	$S_I$	$S_{II}$	$S_{III}$	$S_{IV}$	$S_V$	$S_{VI}$
Voltage	$u_4$	$u_5$	$u_6$	$u_1$	$u_2$	$u_3$

Table 3: Dynamic Switching.

## CHAPTER 5. CIRCUIT IMPLEMENTATION

### 5.1 CIRCUIT TOPOLOGY

#### 5.1.1 PI Controller – DC Link Voltage

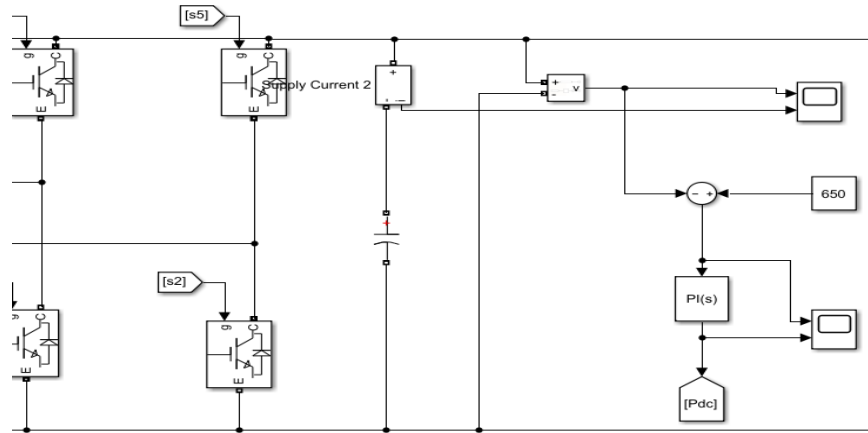


Fig. 5.1 DC Link

The DC Link voltage is being controlled by the help of a PI controller, which stabilizes the Voltage waveform by reducing the error component. It further, reduces the settling time of the system. The PI controller has to keep the DC Link voltage constant in order to ensure perfect operation of the load connected.

The values obtained by trial and error are:  $P=15$ ,  $I = 100$ ;  $V_{ref} = 650V$ . In the final state, the DC Link value, falls into an error band of less than 0.5%, is an excellent control.

#### 5.1.2 LOAD SIDE CONVERTER

To the output side of the DC Link, we have connected an Inverter topology which is acting as a converter between the DC link and the load. This inverter is further connected to an Induction Motor (supposedly an industrial load). This inverter is sometimes called as the load end converter.

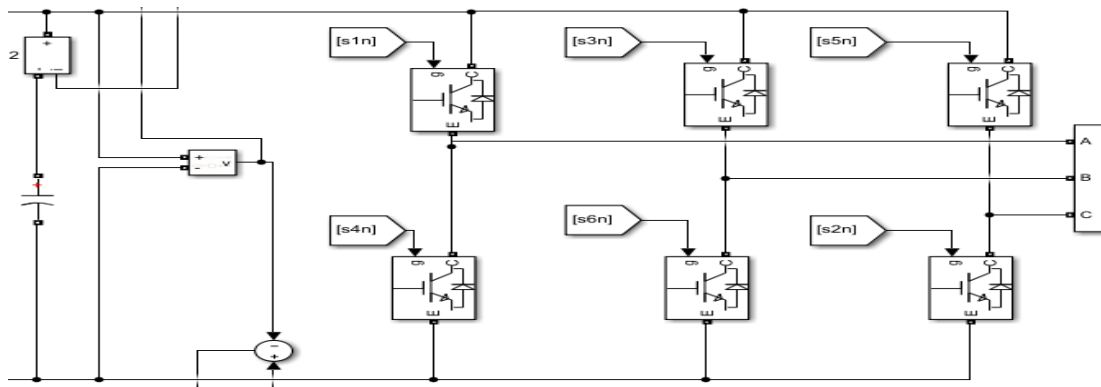


Fig. 5.2 Load End Converter

### 5.1.3 Control of Inverter – SPWM

The inverter connected to the DC Link is controlled through comparison of a high frequency triangle wave with a sine wave, with the sine wave shifted by  $120^\circ$  for each phase respectively.

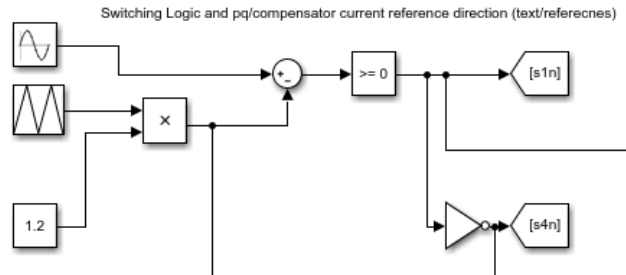


Fig. 5.3 SPWM technique used to trigger the Inverter.

### 5.1.4 Main Load Connected

The primary goal of a front-end converter is to cater to the needs of the Industrial loads by keeping the supply current as close to being sinusoidal as possible. The PCC voltage distortions are to be minimized as well. Here, currently, an Induction motor is used as a load. In the future scope, V/F controlled Induction motor might be used to test the functioning of the entire circuit and all its algorithms.

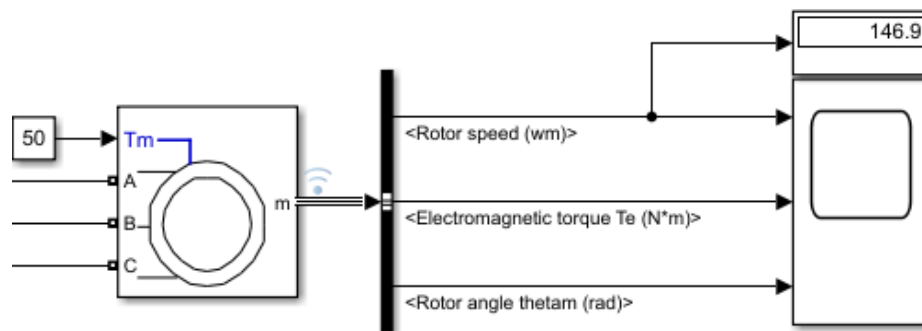


Fig. 5.4 -  $\Theta$  Induction Motor connected as a primary load.

### 5.1.5 Operation in transient condition

In order to test the robustness of the circuit simulation, there are certain transient conditions which are tested to understand about how well the circuit responds to the variation of parameters like the load resistance/inductance, addition of a non-linear load in the circuit, changing torque requirements of the motor, etc.

The results for the same will be attached along with the simulation circuit.

It will be noteworthy to observe the variation in the adaptive gain algorithm resulted due to addition of extra load – which is a being done to protect the switches from over current.

### 5.3 SIMULATION CIRCUIT

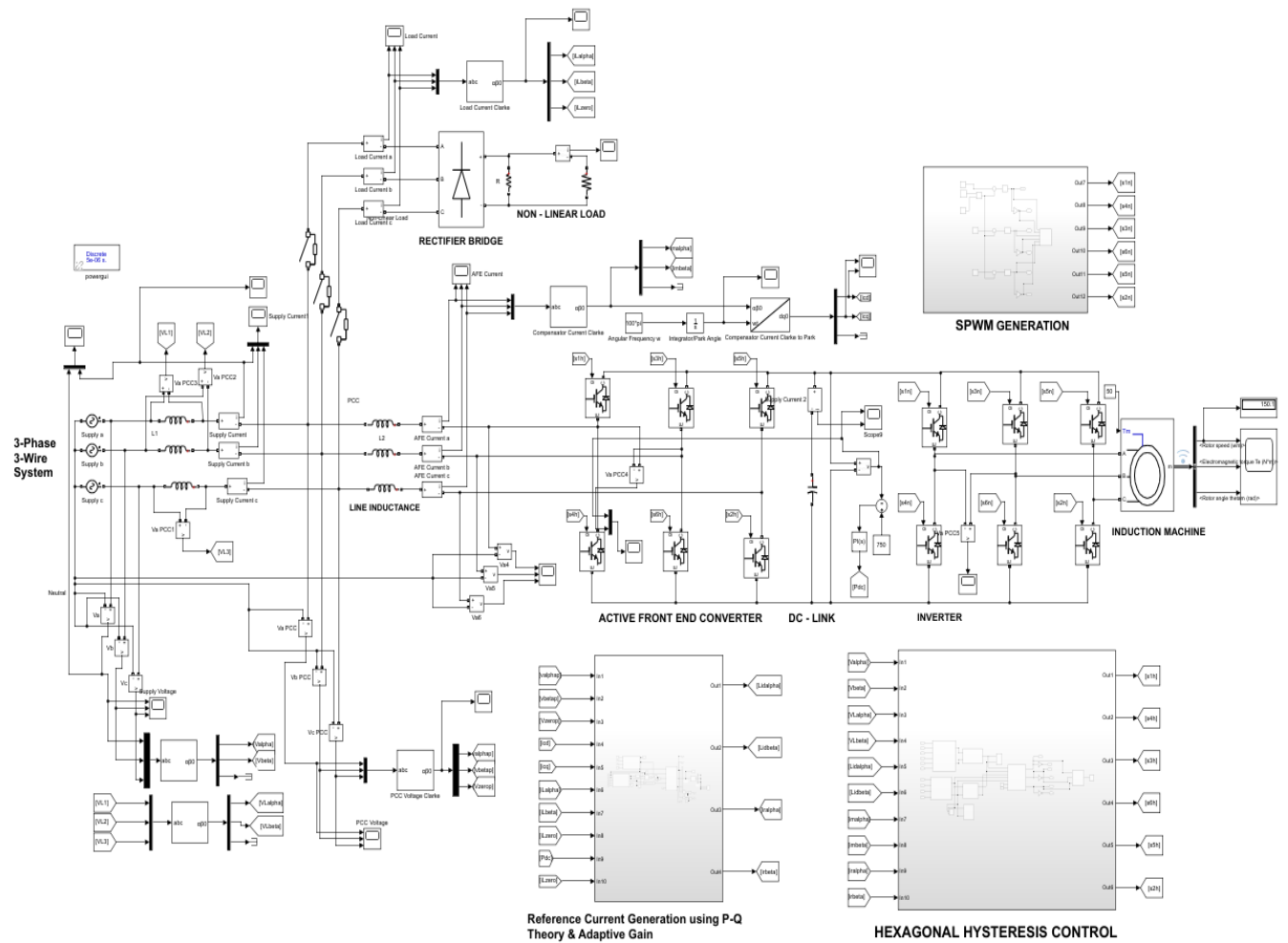


Fig.5.5 Complete Simulation Circuit in MATLAB/Simulink Environment

### 5.2 DESIGN SPECIFICATIONS:

Supply Voltage	230 V
Grid frequency	50 Hz
Load: Induction Machine (triggered by SPWM)	10 HP (7.5 kW) 400 V 50Hz
Load Parameters	1440 rpm
Line Inductance $L_1$	1 $\mu$ H
Line Inductance $L_2$	1 mH (Hexagonal Controller) 5 mH (Adaptive Controller)
DC Link voltage $V_{dc}$	750 V
Fixed Hysteresis bandwidth:	0.5
Adaptive Hysteresis parameter a	0.4 - 0.5
Hexagonal Hysteresis: $\Delta$	0.75, 1 (value increases as load increases)
H	1, 1.5 (value increases as load increases)

## 6. SIMULATION RESULTS

### 6.1. Fixed Band based Hysteresis Current Controller:

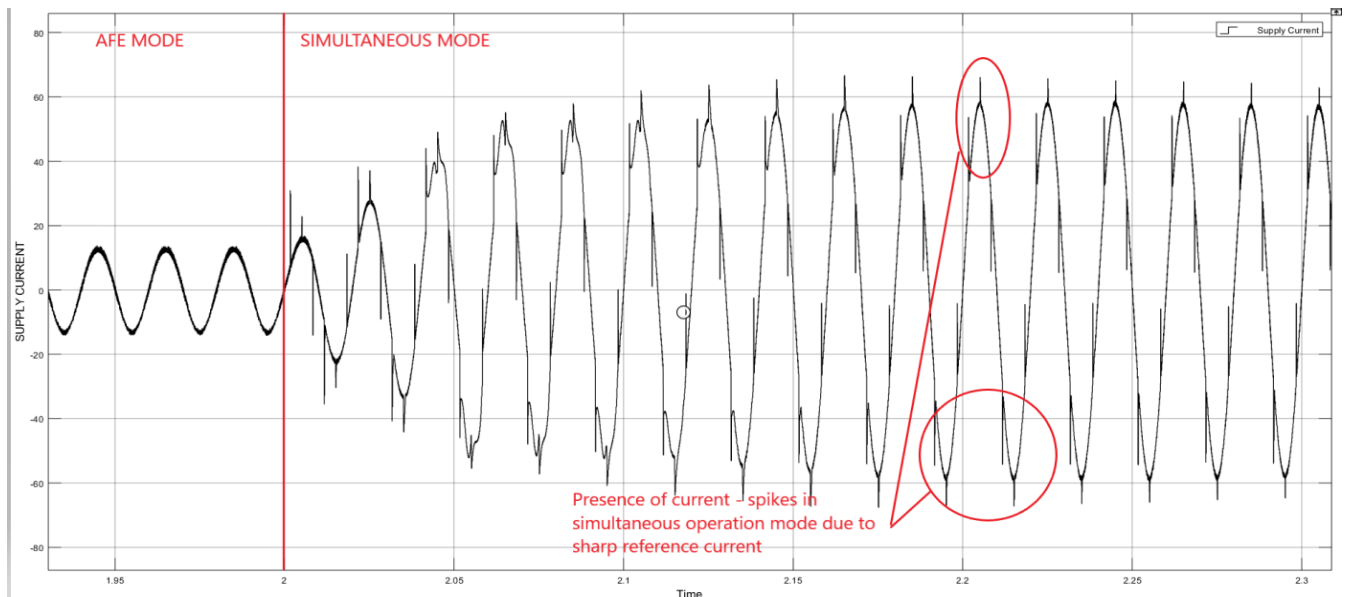


Fig. 6.1.1 Supply current waveform

The supply current is almost sinusoidal for normal AFE operation, during transient state, the waveform becomes distorted for a few cycles, but soon as the circuit starts to settle, the new current which is also sinusoidal in nature (except it is with some spikes of about 65 A on a peak value of 60 A) is seen.

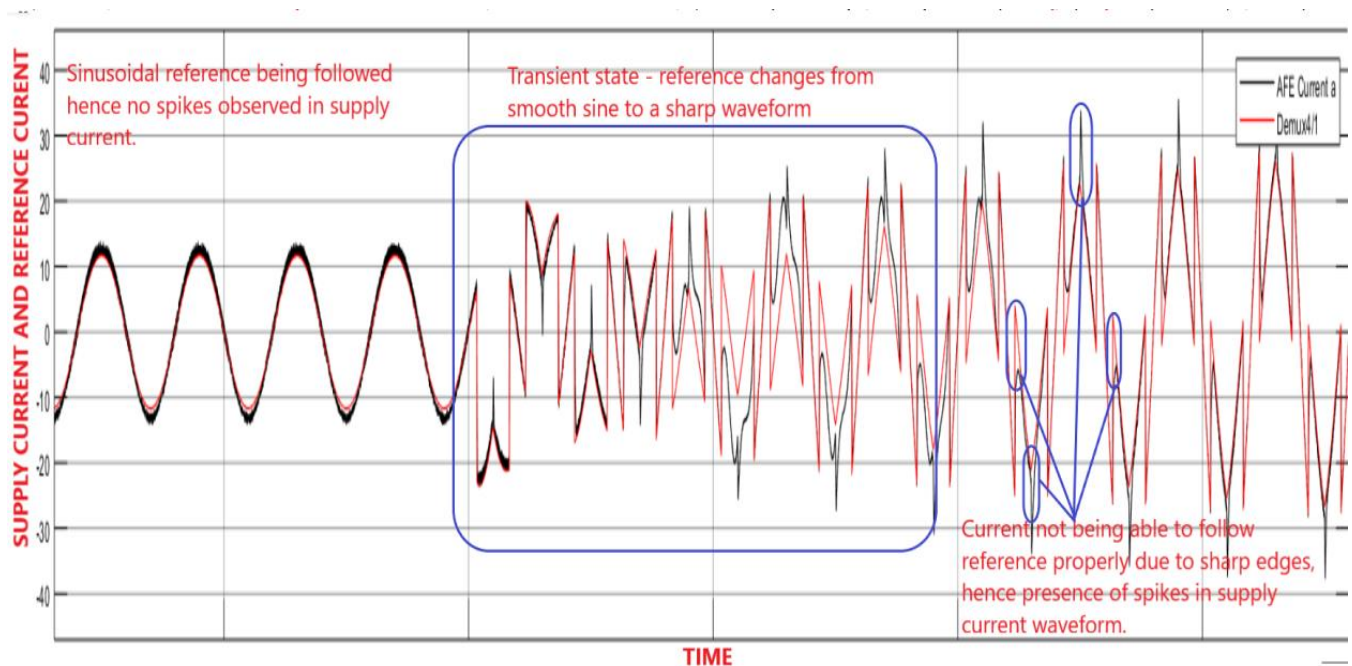


Fig. 6.1.2 Measured current vs Reference current

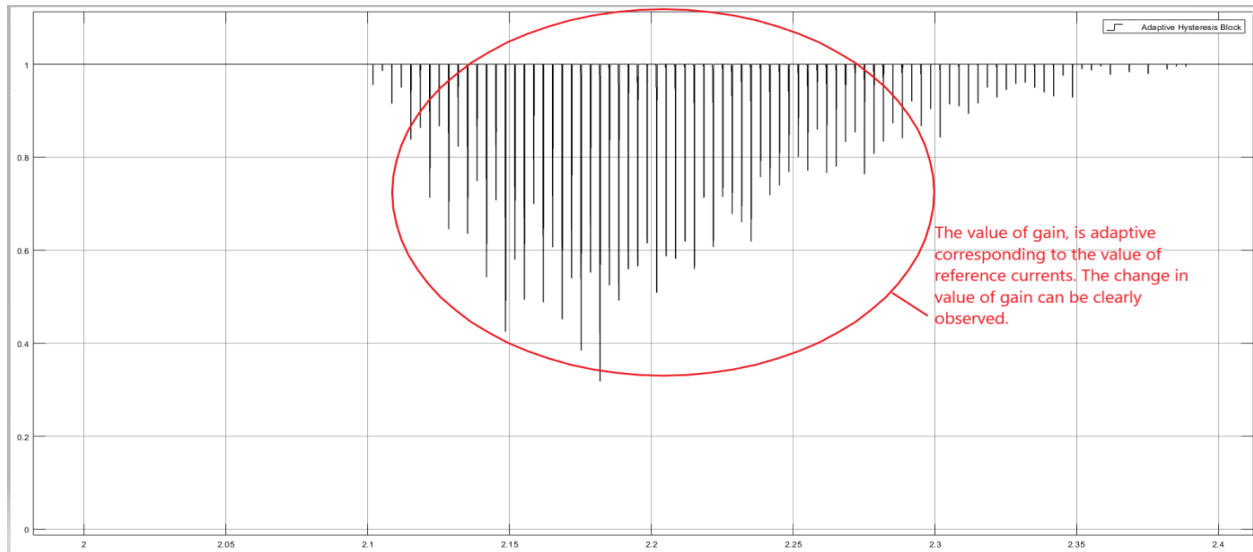


Fig.6.1.3 Adaptive Gain Algorithm Output

The reduction in the value of gain can be seen post  $t=2$  sec when the DC link is not yet stabilized and hence the operation of converter has to be such that more power is supplied to stabilize the DC link voltage and hence the gain is reduced to keep the value of current within limits of switches as specified by the manufacturer.

## **6.2. Adaptive Band based Hysteresis Controller:**

The operation of AFE is changed to simultaneous mode at  $t = 2$  sec after the breaker is switched.

It can be clearly visualised that the operation of converter is like that of AFE before the Non-Linear load is connected – by the sinusoidal reference generated. AT  $t=2$ , as the breaker connects the non-linear load, the system starts acting like a Shunt Active Power Filter as well as AFE.

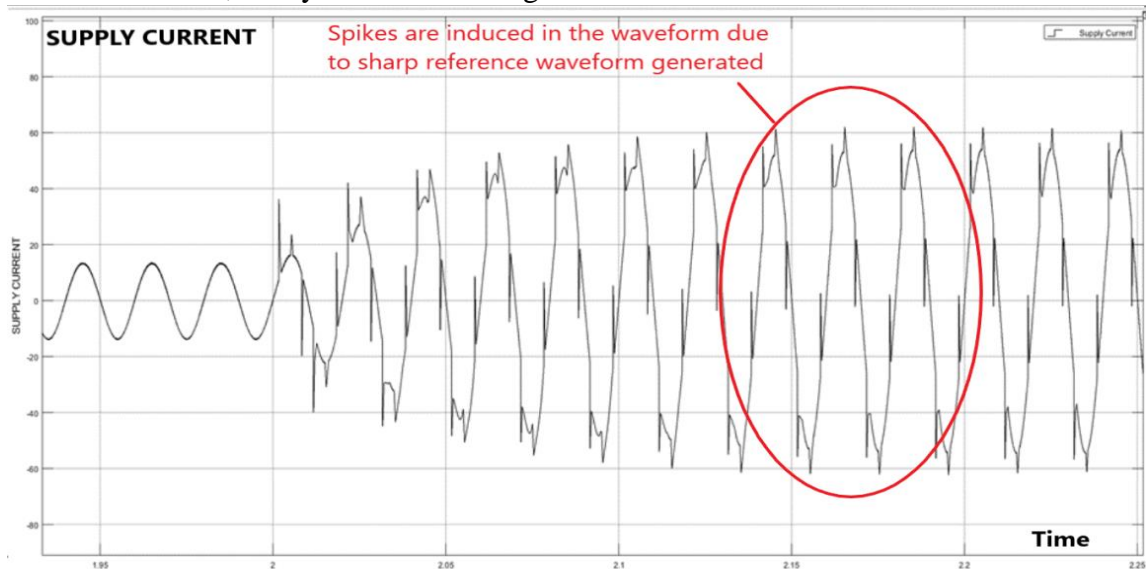


Fig. 6.2.1 Supply current waveform



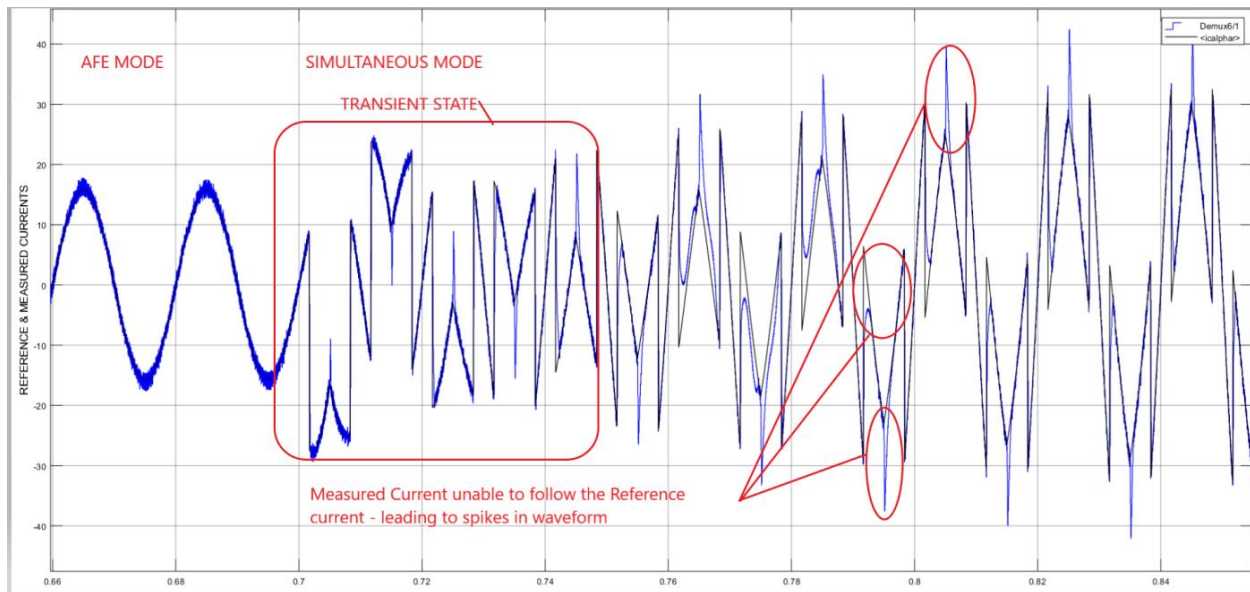


Fig. 6.2.2 Measured current vs. Reference current

It can be clearly observed that at points where the measured current fails to follow the reference currents (at the points showing high/step change), the error becomes quite large for those points and consequently, the Hysteresis band has high peaks. Ideally, there should be no such spikes.

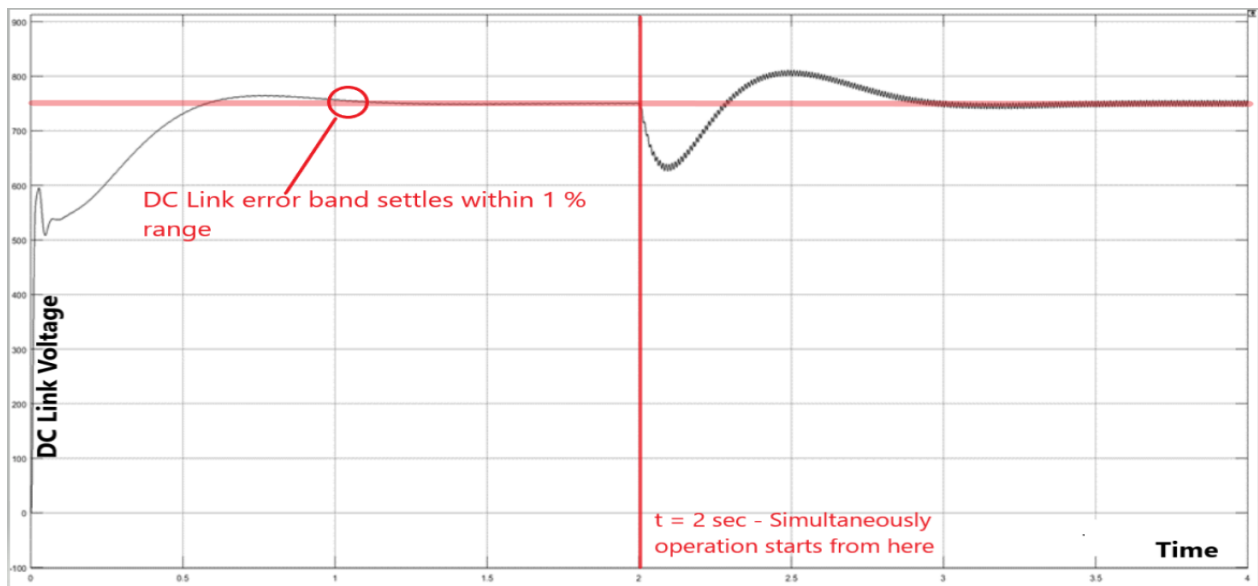


Fig. 6.2.4 (a) DC Link Voltage Profile.

Irrespective of the loading condition, the output value of dc-link voltage is almost a constant value with less than 1% ripple which has been shown in figure.

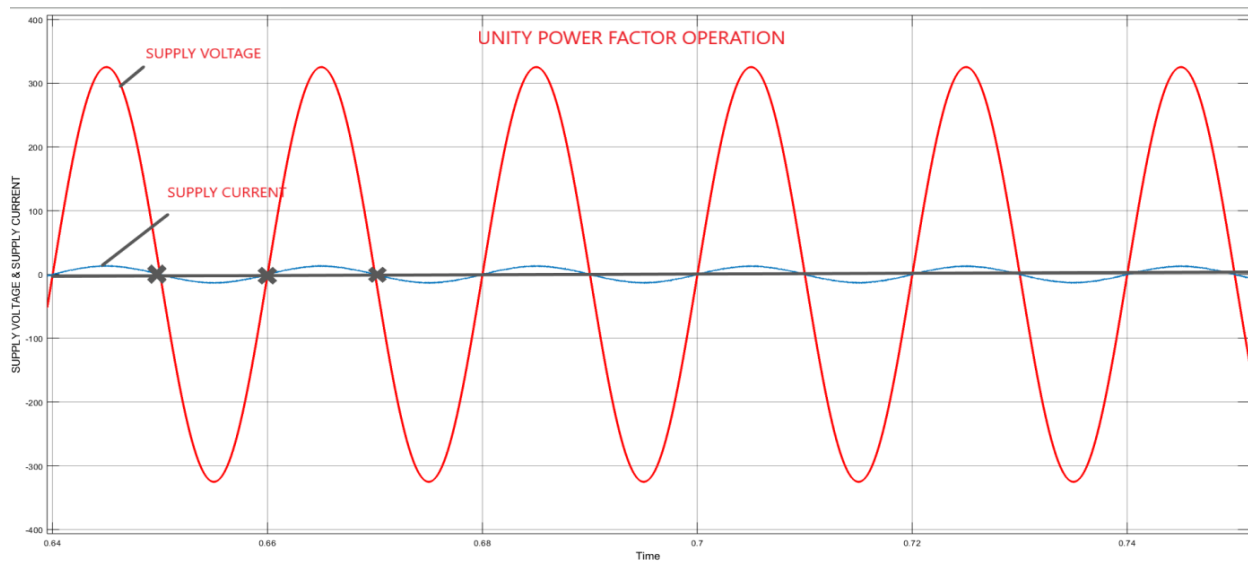


Fig. 6.2.5 Supply Voltage & Current waveform – UPF Operation.

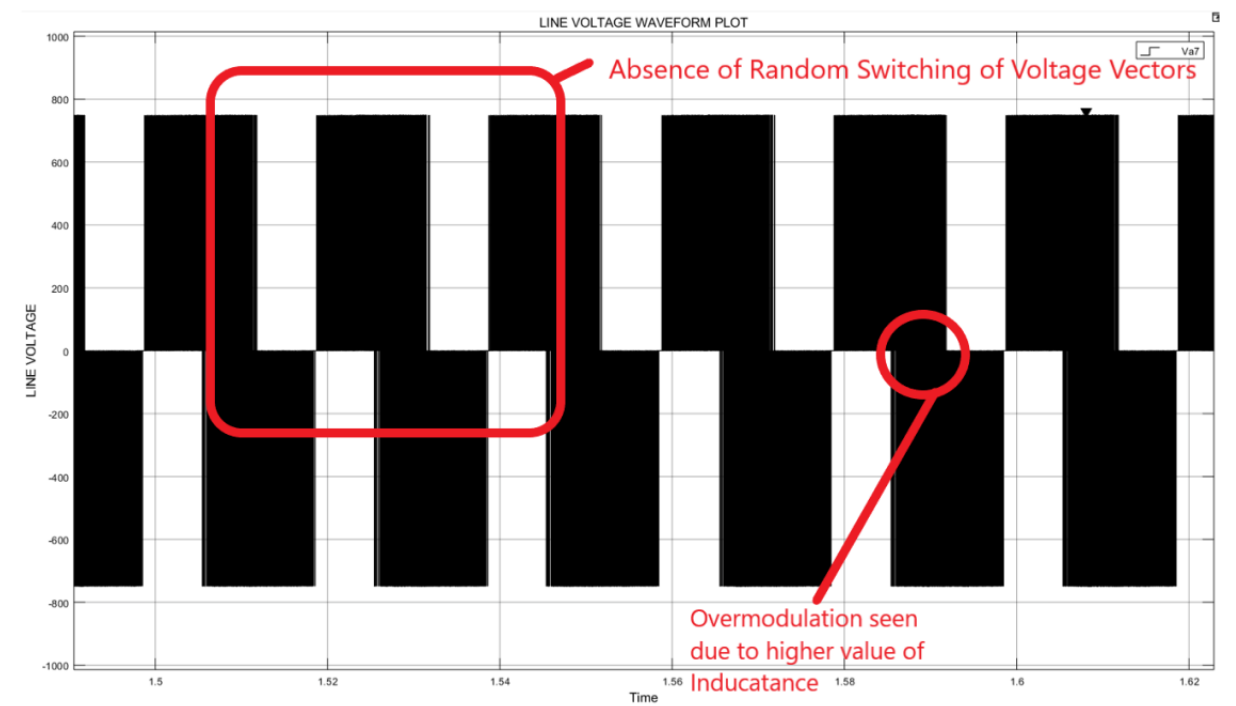


Fig. 6.2.6 Line Voltage Waveform

The line voltage waveform is free from the effects of random switching, however there is a problem of over modulation. The over modulation can be reduced by reducing the value of Line Inductance, but that results in distortion of supply current waveform.

### **6.3 Current Error based (Hexagonal Band) Current Controller**

#### **Results for AFE Mode of Operation:**

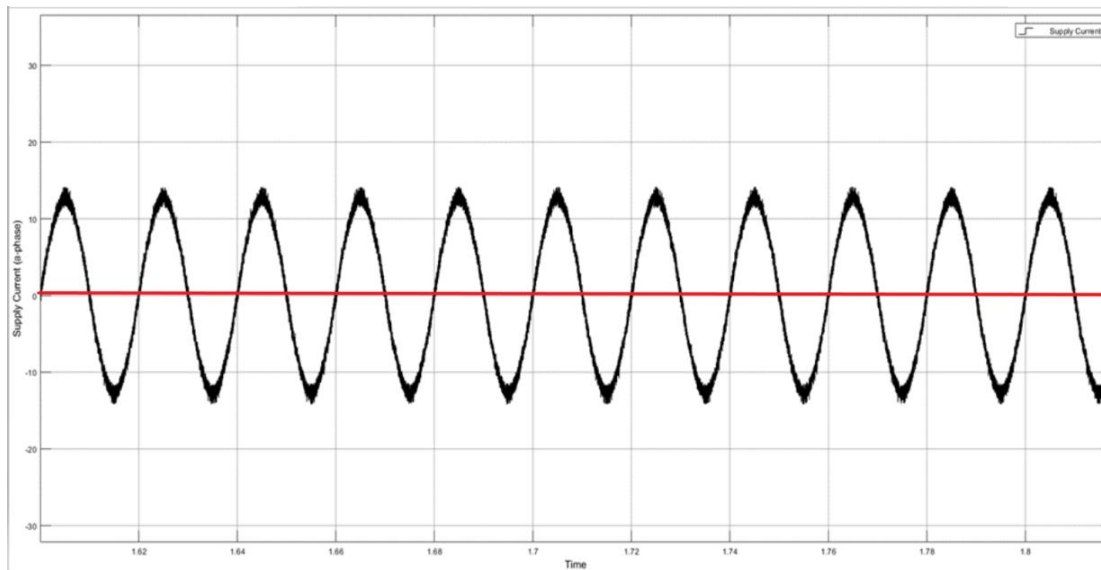


Fig. 6.3.1 Supply Current Waveform (a-phase)

An almost sinusoidal supply current has been observed. The current waveform observed has half-wave symmetry as well as same positive and negative values of peak currents.

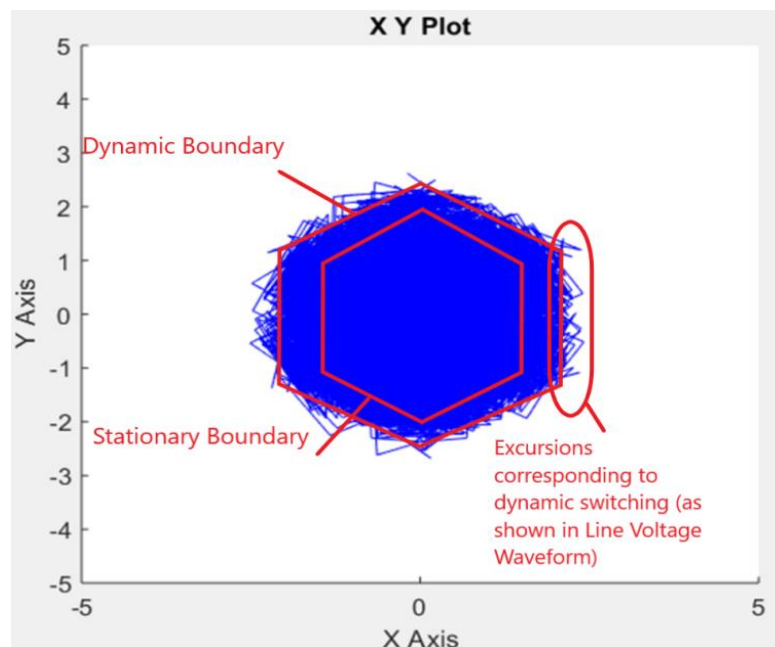


Fig. 6.3.2 XY Plot of  $i_{a\alpha}$  (x-axis) and  $i_{b\beta}$  (y-beta) – Hexagonal Hysteresis Band.

The current error space phasor is seen to be bounded by the Hysteresis Hexagonal boundaries, with minimum distortions by crossing of boundaries.



Fig. 6.3.3 Line Voltage Waveform.

The line voltage waveform observed has very low levels of non-adjacent switching states, and is free from over-modulation.

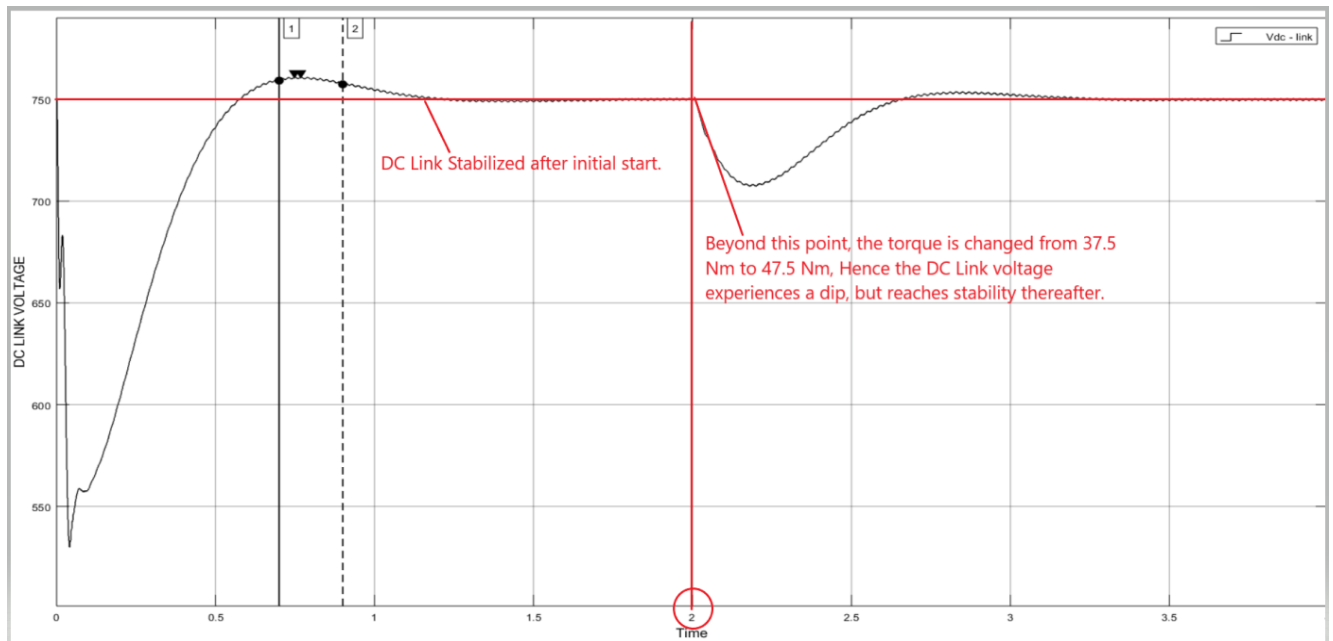


Fig. 6.3.4 (a) DC Link Voltage Profile

The enlarged DC Link waveform is shown; it can be seen that the waveform settles to the reference voltage value with 1% error band, and again settles for the same after a transient condition is achieved.

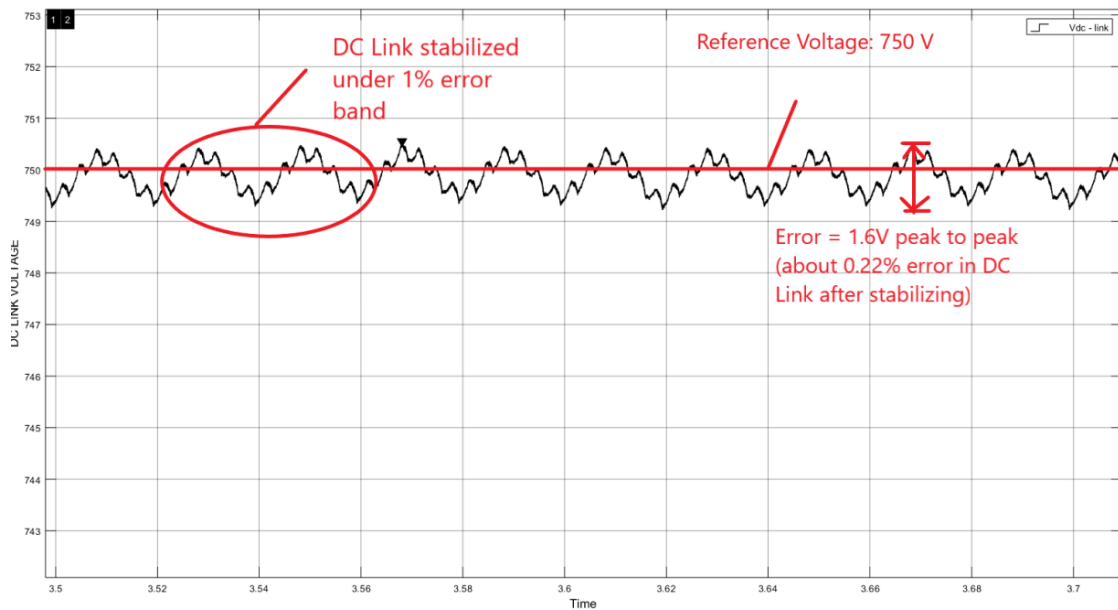


Fig. 6.3.4(b) DC Link voltage after settling time

DC Link settled under 1% error band is shown. This has been achieved by fine tuning of the PI controller. The voltage levels are almost constant.

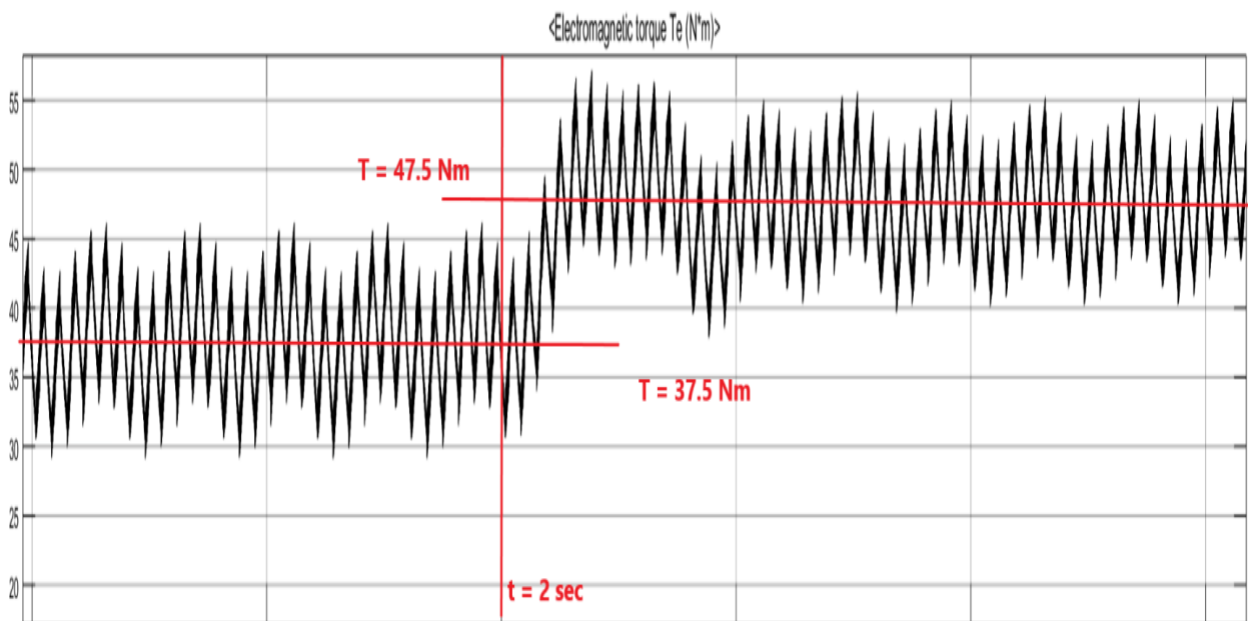


Fig. 6.3.5 Load Torque Variation at  $t = 2$  sec.

The torque can be seen to be varying in a particular contained range.

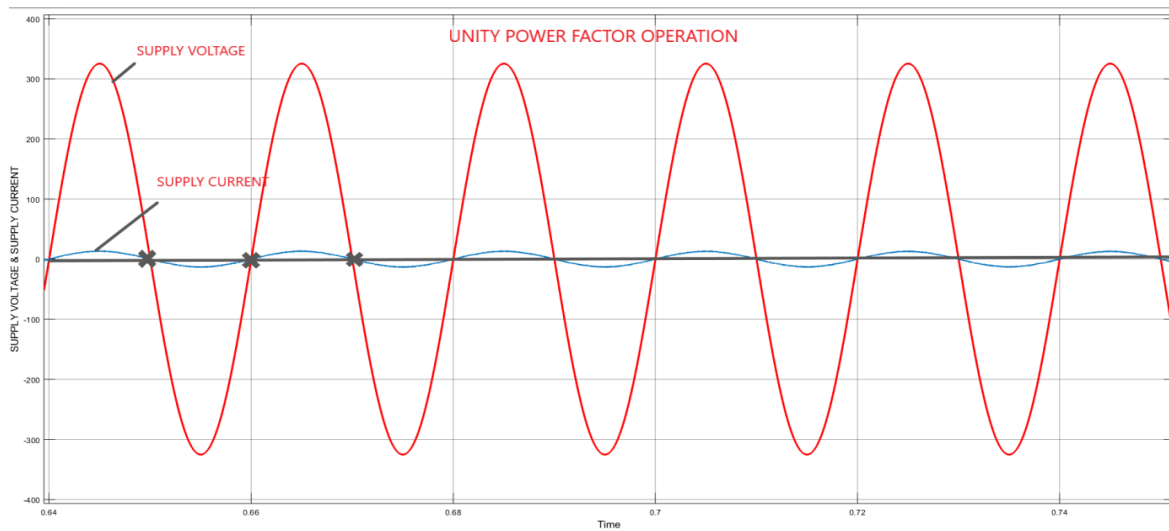


Fig. 6.3.6 Unity Power Factor Operation

UPF operation can be clearly visualized. The supply current and supply voltage are completely in phase. Thus, just like conventional and adaptive hysteresis methods, the hexagonal control method also makes the circuit to operate at Unity Power Factor.

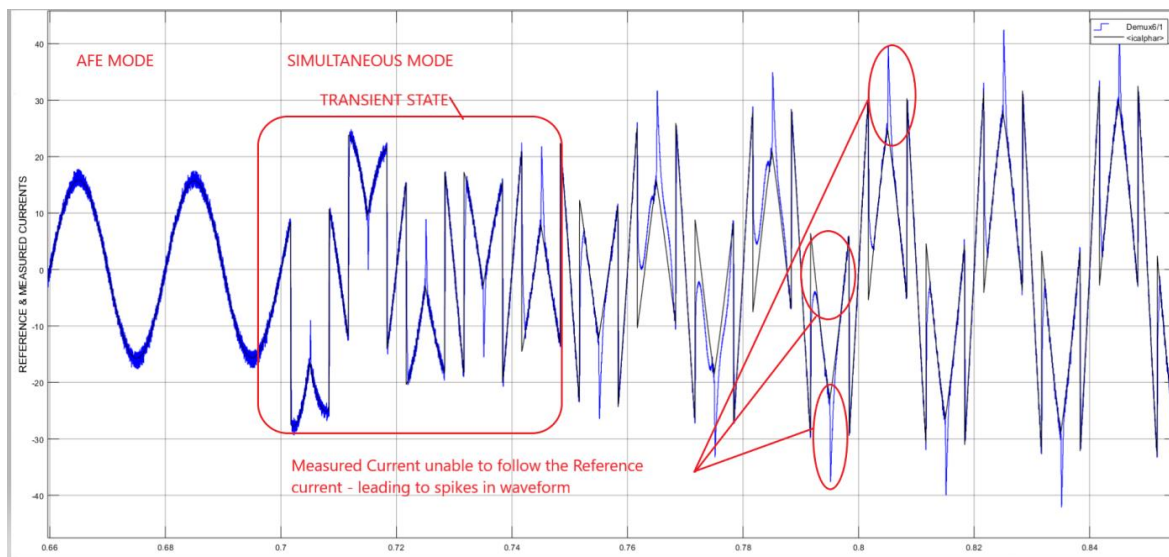


Fig. 6.3.7 Three phase Sinusoidal reference currents when the mode of operation is changed from AFE mode to Simultaneous operation as AFE and SAPF

The change in reference currents waveform from a smooth sinusoidal wave to a sharp (MW) shaped curve can be seen at  $t=0.7$  sec corresponding to the addition of non-linear load; which lead to the operational change of AFE to act as a SAPF as well. This explains the sharp peaks (of up to 42 A) which are observed in the supply current waveforms. This challenge has not been overcome even by the hexagonal hysteresis current control algorithm

## 7. COMPARATIVE ANALYSIS:

The methods of conventional and current error space phasor-based hysteresis controllers are basically methods involving fixed band controllers, and hence they suffer from a common disadvantage, which is variable switching frequency. This leads to sub-harmonics in the line current. Variable switching frequency can be controlled by using variable parabolic bands in the hysteresis controllers. [7]

**7.1 Line Regulation:** The above circuit's operation is tested against the line voltage variation of  $\pm 20\%$  i.e. the Supply voltage ( $V_s$ ) is varied from 230 V to 200 V, to check the behavior of controller for under voltage operation and from 230 V to 270 V for over voltage operation.

In both the cases, controller is able to maintain unity power factor operation i.e. supply current ( $I_s$ ) and  $V_s$  at line side are in same phase. Moreover, load voltage and load current values remain constant irrespective of under voltage and over voltage situations encountered at the grid side. The DC link also settles at reference voltage.

**7.2 Load Regulation:** The above circuit is also simulated with a stepped torque input applied to the induction motor, and even in case of such a load regulation the performance is satisfactory and THD remains well below its limit as specified by IEEE standards. The controller is also able to sustain unity power factor whilst the load changes.

**7.3 THD values for various control techniques:** By reducing the hysteresis band, more and more sinusoidal-natured line current can be achieved with higher switching frequency of the converter. In actual practice, there has to be a trade-off between selection of switching frequency and the quality of the input current waveform.

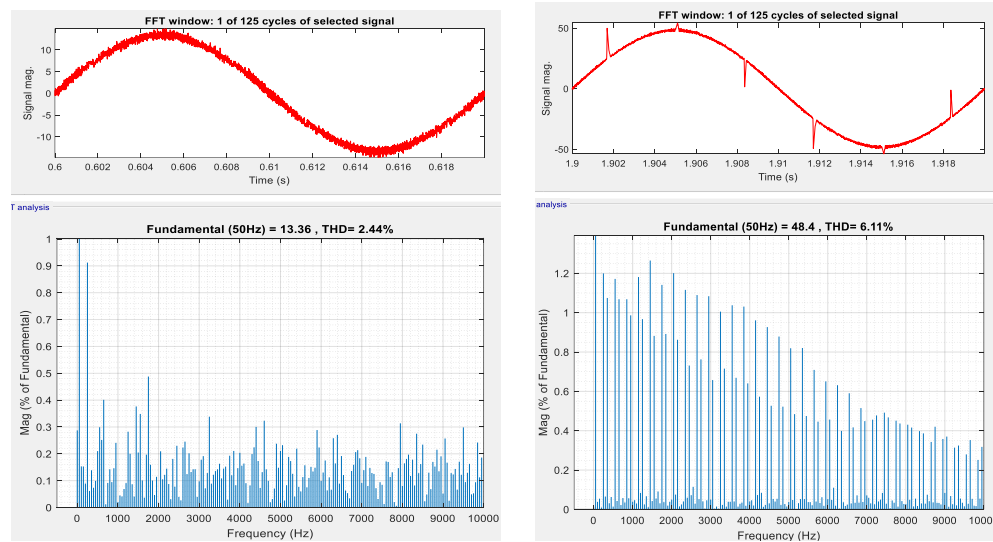


Fig. 7.1 Total Harmonic Distortion for Conventional Hysteresis

The conventional hysteresis has a major disadvantage that the error band remains constant for all the values of load currents, hence the error is highly dependent on load parameters. From the THD comparison, it can be seen that the adaptive algorithm, is better suited for AFE operation, as it is very simple to implement compared to the Hexagonal Hysteresis Control, however, in



cases where the operation is supposed to be simultaneous, the Hexagonal control has better THD reductions.

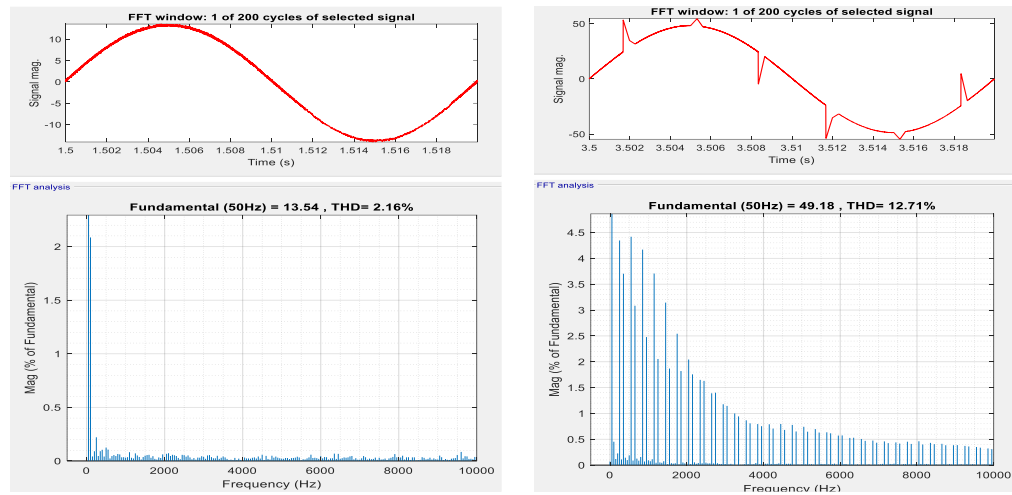


Fig.7.2 Total Harmonic Distortion for Adaptive Hysteresis  
(a) AFE mode – 2.16% (b) Simultaneous Mode – 12.71 % (Above Limits)

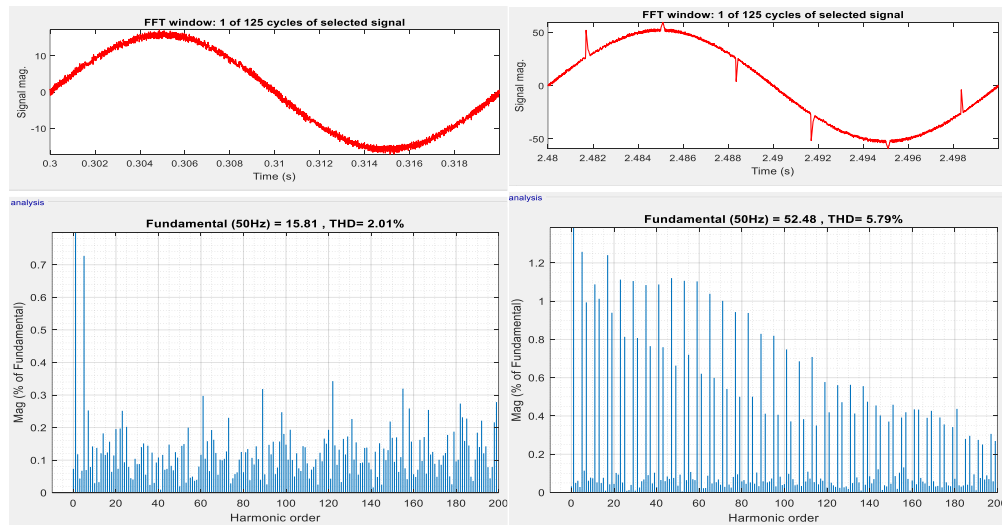


Fig. 7.3 Total Harmonic Distortion for Hexagonal Hysteresis  
(a) AFE mode – 2.01% (b) Simultaneous Mode – 5.79%

There is a significant reduction in the harmonic spectrum as compared to the Adaptive operation, even for the AFE mode as can be compared from Fig. 7.2 (a) where the magnitude levels of dominant harmonic is about 2% whereas it is only about 7% for Hexagonal Hysteresis Control.

Current Controller	AFE Mode	Simultaneous AFE and SAPF
Conventional Hysteresis	2.44%	6.11%
Adaptive Hysteresis	2.16 %	12.71 % (Too High)
Hexagonal Hysteresis	2.01 %	5.79 %

Table 5: Comparison of THD values



## **9. CONCLUSION**

Vector control of active front-end converters has been implemented successfully. The project uncovered various strategies which were analyzed and implemented in succession to tackle the disadvantages of the primitive techniques. The project which saw the implementation of Active Front-End Converter simultaneously working as Active Filter for a non-linear parallel connected load. The basic operation included compensating the Supply current waveform which was non-sinusoidal because of presence of harmonics. The DC link power compensation was taken into consideration and the simulation verified apt compensation of the DC Link, with an error margin of less than 1 %. To ensure that the DC-link compensation, which was the main role of the AFE converter is prioritized over compensation of Non-Linear load in case the current values exceed the switch ratings. The reference compensating currents were generated by implementing the pq-theory of power compensation, which generates a sinusoidal reference for operation of the converter as an AFE. The current was forced to follow the reference by using hysteresis current control techniques. The performance of the controller has not been improved by using an Adaptive Gain Strategy, wherein THD =6.11% still persists, the reason being the presence of current errors.

The conventional hysteresis techniques were quite easy to implement, but posed problems like varying switching frequency and controller not being able to provide desired control levels for loads other than rated loads, as the hysteresis bands remained constant for overall operation.

This challenge was tackled by implementing a constant frequency strategy, known as Adaptive Hysteresis Current Control, where the Hysteresis bands were not constant, but rather dependent on load current values, varying in sinusoidal fashion, which further improved the supply current waveform. This ensured that the THD levels (2.16% for AFE mode) were lower than earlier, but the operation still required higher values of switching frequency, which lead to more prominent switching losses. Also, the line voltage waveform shows overmodulation due to higher value of inductance. Next is to improve the performance of AHCC by using the Hexagon based current error predictive control so as to meet the THD requirements as per IEEE standards. AHCC will be utilizing the current error minimization technique by using vector-based HCC method.

Finally, a more advanced and optimized technique – Hexagonal Hysteresis Current Control was implemented, which gave a better and refined result (THD levels of 1.59%), with reduction in low order harmonic spectrum. This technique, which is implemented in  $\alpha\beta$  reference frame, bounds the current error space phasor within its boundaries.

**FUTURE SCOPE:** A hardware implementation of the circuit had been done and results have been verified. The project has a vast future scope in power systems and can be extended to multi-level converters to further improve the waveform quality. The control strategy can be extended to include additional optimising parameters associated with the localised power system network that the AFE is compensating. Also, with the increased usage of Artificial Neural Networks, the current controller can be modified by using various tools of ANN like NF Tool (in-built in MATLAB) or codes can be written which can further enhance the results.

## REFERENCES

- [1] B. K. Bose *Modern Power Electronics and AC Drives (Book)*
- [2] *Control of front-end Converter with Shunt active Filter using adaptive gain* Hong Viet Luu Alfred Punzet, Volkmar Müller, Ngoc Lan Phung, DRESDEN UNIVERSITY OF TECHNOLOGY Mommsen Strasse 13, D-01062 Dresden, Germany. ISBN: 90-75815-08-5.
- [3] *Converter Simultaneously as Active Front End and as Active Filter*, A. Ndokaj and A. Di Napoli Roma Tre University, Dept. of Ind. and Mecc. Engineering, (Italy), 978-1-4673-4430-2/13/\$31.00 ©2013 IEEE. (Paper)
- [4] *Modelling and Analysis of Electrical Machines by Mrittunjay Bhattacharyya (Book)*
- [5] *Vector control of three-phase AC/DC front-end converter*, J S SIVA PRASAD, TUSHAR BHAVSAR, RAJESH GHOSH and G NARAYANAN Department of Electrical Engineering, Indian Institute of Science, Bangalore 560 012. Sadhana Vol. 33, Part 5, October 2008, pp. 591–613. (Paper)
- [6] Marian P. Kazmierkowski, Ramu Krishnan, Frede Blaabjerg, J. D. Irwin-*Control in Power Electronics\_ Selected Problems (Academic Press Series in Engineering) (2002)*
- [7] Manisha Shah, P.N Tekwani, “Current Error Space Phasor Based Hysteresis Controller Applied to Bi-Directional Front-End Boost-Converter for Unity Power Factor and Low THD
- [8] *Istantaneous-Power-Theory-and-Applications-to-Power-Conditioning* Akaqi-H.-Watanabe-E.-H.-Aredes-M.
- [9] L. Malesani, P. Mattavelli, “Novel Hysteresis Control Method for Current- Controlled Voltage-Source PWM Inverters with Constant Modulation Frequency”, *IEEE Transaction on Industry Applications*, Vol. 26, No. 1, January/February 1990., pp. 88-92
- [10] Mirjana Milosevic “Hysteresis Current Control in Three-Phase Voltage Source Inverter”.
- [11] W. McMurray, “Modulation of the chopping frequency in dc choppers and inverters having current hysteresis controllers,” *IEEE Trans. Ind. Applicat.*, vol. IA-20, pp. 763–768, July/Aug.
- [12] I. Nagy, “Novel adaptive tolerance band based PWM for field-oriented control of induction machines,” *IEEE Trans. Ind. Electron.*, vol. 41, pp. 406–417, Aug. 1994
- [13] M, Shree Harshitha H Dawnee, S Kumaran, Sri Kodeeswara “Comparative Study of Fixed Hysteresis Band Current Controller and Adaptive Hysteresis band Current Controller for Performance Analysis of Induction Motor” 2017 International Conference on Energy, Communication, Data Analytics and Soft Computing (ICECDS)
- [14] Suhara E M, M Nandkumar “Analysis of Hysteresis Current Control Techniques for Three Phase PWM Rectifiers”